

May 7, 2019

Effect of Biodiesel on Polyamide-6 Based Polymers

Jianwei Zhao and P.K. Mallick⁽¹⁾

Department of Mechanical Engineering
University of Michigan-Dearborn, MI, 48128

ABSTRACT

Biodiesel is considered one of the best alternative fuel sources in the transportation industry, but it has shown aggressive characteristics on materials that are used in fuel storage and delivery systems in vehicles. In this study, the effect of biodiesel (B100) on the properties of two polyamide-6 based semi-crystalline polymers was studied and compared with that of diesel and a 20/80 blend of biodiesel and diesel (B20). Experiments were conducted using room temperature immersion tests in the three fuels for 720 hours followed by post-immersion thermal and mechanical tests. In all three fuels, the polymers exhibited non-Fickian weight increase during immersion and did not achieve equilibrium level of absorption in 720 hours. The glass transition temperature (T_g), yield and tensile strengths, storage modulus and peak $\tan \delta$ decreased after immersion, while the degree of crystallinity and loss modulus increased. FTIR study showed that no chemical changes occurred due to immersion. It is concluded that all three fuels absorbed into the polymers acted as plasticizers which caused the observed changes in the properties of the two polymers investigated in this research.

This is the author manuscript accepted for publication and has undergone full peer review but has not been through the copyediting, typesetting, pagination and proofreading process, which may lead to differences between this version and the Version of Record. Please cite this article as doi: [10.1002/pen.25131](https://doi.org/10.1002/pen.25131)

Key Words: Polyamide-6, biodiesel, diesel, dynamic mechanical properties, tensile properties, crystallinity, FTIR

(1) Corresponding author: Ph. 313-593-5119

E-mail: pkm@umich.edu

Author Manuscript

1. INTRODUCTION

Polymers are used in many fuel container and fuel delivery applications where they are exposed to or immersed in fuels that can cause degradation in their physical and mechanical properties. The degradation may take place immediately or over a period of time. Richaud et al. [1] divided the effect of polymer-fuel interactions into two main categories: physical and chemical, both occurring as a result of diffusion and absorption of the fuel into the polymer. The physical interaction may cause stress cracking on the polymer surface, alter physical and mechanical properties or extract performance-enhancing additives used in the polymer, but no chemical modifications of the polymer molecules. The chemical interaction, on the other hand, may cause oxidation or hydrolysis of the polymer molecules due to the reaction with functional groups, such as esters and amides, that may be present in the fuel.

In recent years, biodiesel has emerged as one of the primary alternative fuels for diesel engines. Biodiesel comprises of fatty acid methyl esters (FAME) derived from vegetable oils, animal fats or recycled greases [2-5]. It is used either as 100% FAME, often designated as B100, or in lower volumetric concentrations in which it is blended with diesel, such as a B20 blend in which 20% biodiesel is blended with 80% diesel. Biodiesel has several advantages over diesel, such as high combustion, lower carbon-dioxide emission, sustainability, biodegradability and eco-friendliness. Because of these advantages, it is considered an excellent fuel for both city and highway driving of automobiles and other vehicles. However, compared to traditional diesel, biodiesel shows much more aggressiveness on fuel storage and

delivery systems. For example, it can be highly corrosive on metals used in vehicle fuel lines [6], and when exposed to air during long-term storage, biodiesel tends to oxidize which increases its acid content and in turn, increases the corrosion rate. Similarly, traditional elastomers used in fuel line hoses, gaskets and O-rings are also shown to degrade by swelling and other physical changes on long-term exposure to biodiesel.

Majority of the studies on the effect of biodiesel on polymers have been conducted with elastomers, such as nitrile rubbers, fluoro-elastomers and silicone rubber that are used in today's diesel engines [7-13]. The changes in the physical and mechanical properties of these elastomers after immersion in biodiesel were attributed to chemical changes, such as the generation of functional groups, additional crosslinking and chain scission. There are fewer reported studies in which the effect of biodiesel on thermoplastic polymers was considered. Richaud et al. [14] conducted immersion experiments to measure absorption of rapeseed and soy biodiesels in pipe-grade polyethylene films and reported that the amount of absorption increased with increasing immersion time, but reached an equilibrium level of 4.7% in approximately 139 hours at 23°C. The equilibrium concentration increased with increasing temperature. Böhning et al. [15-17] investigated the influence of biodiesel and diesel on tensile and impact properties of several different high density polyethylene (HDPE) grades. They observed significant decrease in modulus, but increase in both tensile failure strain and impact strength, all of which were attributed to plasticization effect of biodiesel absorption in HDPE. Lutz and Mata-Segreda [18] reported the immersion experiment results of a highly plasticized polyvinyl chloride (PVC) and two different high-impact polystyrenes (HIPS) in diesel and palm ethyl biodiesel at 20°C. At the end of three months, PVC transformed from a flexible

material to a rigid brittle material due to the loss of plasticizer from it. The diffusion of biodiesel in HIPS depended on the ratio of benzene rings to CH=CH units in the polymer molecules. Ullah [19] examined the effect of B20 blend on the impact strength of a polyoxymethylene (POM) copolymer. The impact strength decreased by 37.5%, which was attributed to the presence of surface cracks generated after 800 hours of immersion. Baleno et al. [20] considered the effect of a B30 blend on the properties of unfilled, glass fiber reinforced and carbon fiber reinforced polyphthalamide. Even after 5,000-hour immersion at 90°C, they did not observe any changes in weight, tensile, flexural and impact properties of these materials. Gomez-Mares et al. [21] conducted immersion tests in diesel and B30 blend for up to 1,008 hours at 120°C using unreinforced and glass fiber reinforced polyoxymethylene, polyphthalamide and polyphenylene sulfide and did not observe much changes in their tensile properties. In another study, Baena et al. [22] evaluated the stability of HDPE, POM and polyamide-66 (PA-66) in palm biodiesel and its blends. After immersion for 14 to 18 hours at 55°C, HDPE and POM did not show any significant changes in mechanical properties, but PA-66 had a significant decrease in tensile strength. However, FTIR study showed that there were no appreciable changes in the chemical structures of these polymers. The changes in mechanical properties were explained as mainly due to physical absorption of the fuels into the polymers.

The objective of the current research is to determine the effects of biodiesel on the properties of two polyamide-6 based polymers that may find applications in fuel tanks, fuel flow lines and fuel distribution systems in road vehicles. Currently, the polymer used for gasoline fuel tanks is high density polyethylene (HDPE). However, since HDPE has a relatively high permeability for gasoline, it is either layered with ethylene vinyl alcohol (EVAL) or cross-linked. Polyamide-6 has a significantly lower

gasoline permeability than HDPE, and therefore, can be used in monolayer. It also has a much higher modulus and strength, and therefore, can be designed with thinner walls. As a result, polyamide fuel tanks can be lighter, and has the potential of being cost competitive with HDPE fuel tanks. As mentioned before, several studies have addressed the effect of biodiesel on HDPE; similar studies on polyamide-6 is lacking. If polyamide-6 is selected for use in biodiesel fuel tanks or other biodiesel storage applications, the effect of biodiesel on polyamide-6 will be of interest.

2. EXPERIMENTAL

Fuels

Three different fuels were used in this research: 100% diesel, 100% biodiesel (B100) and a volumetric blend of 20% biodiesel and 80% diesel (B20). All the fuels were purchased from Iowa Central Fuel Testing Laboratory, Iowa, USA. The biodiesel is reported to be soybean based with an ester content of 97.6% and a moisture content of 0.011%. As shown in Figure 1, the chemistry of biodiesel is very similar to that of diesel. Both contain hydrocarbon molecules, typically 16 carbon atoms long, and except at the ends, two hydrogen atoms are attached to each carbon atom. The biodiesel molecule contains a methyl ester group or COOCH_3 group at one of its ends instead of a methyl group or CH_3 group as in diesel.

Polymers

Two commercially available polyamide-6 based polymers were selected for the immersion tests: Capron 8202, a homopolymer [23] and Capron 8351, a graft copolymer [24]. Both are semi-crystalline polymers and are known to have excellent chemical resistance to oils and hydrocarbons, and are candidates for fuel storage and delivery systems. The copolymer has a higher impact resistance than the

homopolymer. They were supplied by the BASF Corporation in the form of extruded black-pigmented sheets.

Specimen Size

Rectangular specimens cut from the extruded sheets were used in all experiments. The average thickness of Capron 8202 was 1.62 mm and that of Capron 8351 was 1.55 mm. Two different specimen sizes were used: 7 mm x 25 mm for weight measurements and DMA tests, and 14 mm x 50 mm for tension tests.

Specimen Drying

Before the immersion experiments, the specimens were dried in an air-circulating oven at 85°C for 96 hours. The moisture content in the sheets was not directly measured; however, the specimens were dried at 85°C for various lengths of time to remove the absorbed moisture and their weight loss was measured. Drying was continued until the weight loss became stable. It was observed that the weights reduced sharply within the first 24 hours of drying, and tended to become stable at around 2.58% for Capron 8202 and 1.96% for Capron 8351 after 96 hours of drying. Another parameter used in verifying the drying time effect was the glass transition temperature, T_g , which was measured using Dynamic Mechanical Analysis (DMA). For both polymers, T_g increased from 25°C to 65°C after 24 hours of drying. It then increased slowly and tended to stabilize at 70.77°C for Capron 8202 and 70.20°C for Capron 8351. The increase in T_g can be attributed to desorption of moisture in the polymers. Following these two experiments, all specimens were oven-dried at 85°C for 96 hours before conducting the immersion experiments.

Immersion Experiments

The dried specimens of Capron 8202 and 8351 were immersed in sealed glass containers filled with diesel, B20 and B100 fluids at 25°C for up to 720 hours. Specimens were taken out from the container at regular time intervals to measure their weight change. Several dried specimens of Capron 8202 and 8351 were immersed under stress in all three fluids at 25 °C for 720 hours. In the stressed immersion tests, specimens were held in a bent configuration in a 37 mm wide C-channel, as shown in Figure 2. Specimens were removed from the containers and released from the C-channel after 720 hours.

It is assumed that the specimen inserted in the C-channel is part of a circle as shown in Figure 2. Assuming an elastic deformation, the tensile strain on the top outside surface of the stressed specimen is $\varepsilon = \frac{h}{2R}$, where h is the specimen thickness and R is the radius of curvature, which was calculated to be equal to be 19.13 mm. Since the thicknesses of Capron 8202 and Capron 8351 specimens were 1.62 mm and 1.55 mm respectively, the corresponding tensile strains were 4.23% and 4.05%. The estimated tensile yield strains from the manufacturer's published data are 2.8 and 3.3%, respectively. Thus, the tensile strains in the stressed specimens were slightly higher than the yield strains of the polymers. The reported failure strains of both polymers is 50% or higher [23, 24].

Post-Immersion Experiments

After immersion, specimens were tested to determine the physical and chemical changes that may have occurred due to immersion. The post-immersion experiments included weight measurements, tensile tests, dynamic mechanical analysis (DMA), differential scanning calorimetry (DSC), and Fourier transform infrared spectroscopy

(FTIR).

The specimen weights before and after immersion were measured using an electronic analytical balance, Denver Instrument SI-234, which has a readability of 0.0001 g. Tensile tests were conducted using an INSTRON 4469 materials testing machine. Straight-sided rectangular specimens, 50 mm in length and 14 mm in width, were used. The tests were conducted at a crosshead speed of 2.5 mm/min. The tensile strength was calculated using the maximum load and the yield strength was calculated using the stress at the end of the elastic part of the stress-strain diagram.

Dynamic mechanical properties were measured using a TTDMA (Model No. TRITON T1014231). The specimen was held in a three-point beam bending mode and a loading frequency of 1 Hz was applied at the midlength of the specimen. The temperature ramp rate was 2°C/min and the end temperature was set at 110°C.

The degree of crystallinity C was measured using a differential scanning calorimeter (DSC) (TA instruments SDT Q600). It was determined by analyzing the DSC thermogram during the heating cycle and was calculated using the following equation.

$$C = \Delta H_f(T_m) / \Delta H_f^o(T_m^o)$$

where, $\Delta H_f(T_m)$ is the enthalpy of fusion measured at the melting temperature T_m and $\Delta H_f^o(T_m^o)$ is the enthalpy of fusion of the totally crystalline polymer measured at the equilibrium melting temperature T_m^o . For polyamide-6, $\Delta H_f^o(T_m^o) = 230.1$ J/g, which was used in the degree of crystallinity calculations of both Capron 8202 and Capron 8351. The heating rate was 8°C/min, starting from 25°C and ending at

250°C. The heating thermogram of Capron 8202 exhibited one melting peak at its crystalline melting temperature. The heating thermogram of Capron 8351 exhibited two melting peaks. The larger peak is the primary peak which occurs at the crystalline melting temperature of polyamide-6, whereas the smaller peak is the secondary peak that occurs at the melting temperature of the rubbery phase present in this polymer.

3. RESULTS

Physical Effects

Figures 3 and 4 show percentage weight increase of dry Capron 8202 and 8351 specimens after immersion at 25°C as a function of t , where t is the immersion time in hours. None of the three fuels reached the equilibrium level of absorption in 720 hours of immersion. Among the three fuels considered, the highest absorption was observed in B100 and the lowest in diesel. To determine if the fuel absorption followed the Fickian diffusion model [25], the weight increase data were examined as a function of $t^{0.5}$ and it was observed that it follows a sigmoidal relationship with $t^{0.5}$ instead of a linear relationship, which indicates a non-Fickian diffusion characteristic. It is interesting to note that biodiesel absorption in both Capron 8202 and 8351 after 720 hours was significantly lower compared to HDPE for which the equilibrium level was 4.7%, achieved in approximately 139 hours at 23°C [14].

Table 1 summarizes the weight increases of both Capron 8202 and 8351 specimens after 720 hours of immersion in diesel, B20 and B100 fuels under unstressed and stressed immersion conditions. It can be observed in Table 1 that for both Capron 8202 and 8351 specimens in 25°C immersion tests, the highest weight increase under both unstressed and stressed conditions was in B100, followed by B20 and diesel. Compared to Capron 8202 specimens, the absorption of all three fuels was

lower in Capron 8351 specimens. The weight of the stressed Capron 8202 specimens after 720 hours immersion was higher than the unstressed Capron 8202 specimens. For the stressed Capron 8351 specimens, the weight increase was higher only in B100.

The absorption of all three fuels was also manifested in thickness changes which increased with increasing immersion time and ranged up to 1.85%. Visual observation as well as scanning electron micrographs of the surfaces of immersed specimens did not reveal any anomalous surface characteristics, such as discoloration, voids or fine cracks.

Yield and Tensile Strengths

The yield and tensile strengths of Capron 8202 and 8351 specimens immersed in diesel, B20 and B100 under different immersion conditions are listed in Table 2. For comparison, tensile strength data of both Capron 8202 and 8351 specimens before immersion are also given in Table 2. Each value in the table is an average of three specimens. It can be observed in Table 2 that Capron 8202 had higher strengths than Capron 8351. This is because Capron 8351 is a copolymer containing a randomly dispersed softer phase in the polyamide-6 matrix.

All of the specimens tested in tension failed at locations away from the grips. Figure 5 shows photographs of the failed ends of dry Capron 8202 and 8351 specimens after tensile tests. Ductile failure of both materials tested before immersion and after 720-hour immersion in B100 can be observed in this figure. Similar failure occurred after immersion in diesel and B20. Thus, immersion in all three fuels up to 720 hours did not cause any changes in the failure mode. However, as can be seen in Table 2, both Capron 8202 and 8351 specimens experienced reductions in yield and

tensile strengths after immersion. In general, reduction in yield strength was higher for specimens immersed under stress.

Dynamic Mechanical Properties

Dynamic mechanical analysis (DMA) provided the dynamic mechanical properties, such as $\tan \delta$, storage modulus and loss modulus plots as a function of temperature. From these plots, glass transition temperature (T_g), peak $\tan \delta$, storage modulus at 25°C and loss modulus at 25°C were determined and compared between before immersion and after immersion specimens. Each experiment was conducted in triplicate; the averaged values are given in Table 3.

Figure 6 shows typical DMA diagrams obtained with Capron 8202 and Capron 8351 specimens before immersion. The peak of the $\tan \delta$ curve occurs at the glass transition temperature of the polymer. At this temperature, a large decrease in storage modulus is observed. For Capron 8202, which is a homopolymer, the experiment was conducted from approximately 30°C to 110°C. As can be seen in Figure 6(a), there was a single $\tan \delta$ peak, corresponding to the T_g of polyamide-6 at 72°C. For the Capron 8351 specimen, which is a copolymer, the experiment was conducted from -110°C (using liquid nitrogen) to 110°C. In this case, two $\tan \delta$ peaks were observed (Figure 6(b)). The smaller peak at -60.2°C corresponds to the soft rubbery phase in Capron 8351 and the larger peak at 70.2°C corresponds to the polyamide-6 molecules. The larger peak is considered the primary glass transition temperature of Capron 8351.

Glass Transition Temperature (T_g)

Figure 7 shows that T_g of Capron 8202 and 8351 decreased with increasing immersion time in all three fuels. It can also be seen that for the same immersion time, T_g of Capron 8202 decreased with increasing biodiesel content. Figure 7 shows that T_g of Capron 8351 also decreased after 240 hours of immersion; however, it appears to have leveled off at between 57~58°C.

Peak $\tan \delta$

Figure 8 shows peak $\tan \delta$ of Capron 8202 and Capron 8351 as a function of immersion time. It can be observed that peak $\tan \delta$ of Capron 8202 reduced significantly after immersion in all three fuels. However, changes in peak $\tan \delta$ after 240 hours of immersion were relatively small. The peak $\tan \delta$ of Capron 8351 also decreased significantly and its value became lower with increasing immersion time. It was also observed that the $\tan \delta$ curve was broadened by the absorption all three fuels into both polymers. This is shown in Figure 9 for Capron 8202.

Storage and Loss Moduli

Figure 10 shows the 25°C storage modulus of 8202 and 8351 specimens as a function of immersion time. For both polymers, storage modulus decreased with increasing immersion time. Figure 11 shows the loss modulus changes of Capron 8202 and Capron 8351 after 25°C immersion. For both polymers, the loss modulus increased with increasing immersion time.

DSC Measurements

Figure 12 shows the DSC thermograms obtained during heating and cooling stages for Capron 8202 and 8351 specimens before immersion and after 720-hour

immersion in B100. Similar thermograms were obtained before and after immersions in diesel and B20. From the heating thermograms, the primary crystalline melting peaks for Capron 8202 specimens are at 223.61°C before immersion and 224.49°C after immersion in B100. For Capron 8351 specimens, the primary crystalline melting peaks are at 221.63 and 221.64°C, respectively. In addition to the primary crystalline melting peak, there is an additional melting peak at 96.84°C for Capron 8351 before immersion and 95.65°C after immersion. These secondary melting peaks may be attributed to the melting of the soft phase in Capron 8351. No additional notable features were observed on DSC thermograms of either Capron 8202 or 8351 specimens that can be associated with the effect of immersion in any of the three fuels.

The DSC thermograms provided the information on the degree of crystallinity and the primary melting peak that are listed in Table 4. As can be observed in this table and also in Figure 13, the degree of crystallinity of Capron 8202 was higher than that of Capron 8351. Although the changes in melting peak, T_m , were not significant for either polymer, the degree of crystallinity of both polymers increased slightly with increasing immersion time in all three fuels. However, the increase in the degree of crystallinity of Capron 8351 was much smaller.

FTIR Spectra

Figure 14 shows the FTIR spectra in absorbance mode for Capron 8202 and Capron 8351 specimens before and after immersions in diesel, B20 and B100 under different immersion conditions. All of the spectra show the IR absorbance peaks that are normally found for polyamide-6. A compilation of the observed peaks is given in Table 5 for Capron 8202 and Capron 8351, respectively. This table also lists the

standard FTIR peaks that are used to identify the chemical structure of polyamide-6. By comparing the observed peaks with the standard peaks, it can be concluded that no discernible chemical changes occurred due to the absorption of fuels in the polymers.

4. DISCUSSION

The effect of fuel-polymer interactions can be divided into two main categories: physical interaction and chemical interaction, both occurring due to the diffusion and absorption of fuel into the polymer [1]. Since fuel molecules are much smaller than the polymer molecules, they may be absorbed in the polymer, and act as a plasticizer, altering its physical and mechanical properties, such as modulus, toughness, and strength of the polymer. The direct contact between the fuel and the polymer may cause stress cracking on the polymer surface, which can accelerate fuel penetration into the polymer. Chemical interaction involves modification of polymer molecules. The most possible mechanism for chemical interaction is polymer oxidation, which may or may not accompany fuel oxidation. The existence of moisture in the polymer and the fuel may also cause hydrolysis of polymers that contain functional groups, such as esters, amides and acetals, in their molecules. These functional groups can interact with water molecules to form acid or aldehyde groups. Since some biodiesels contain fatty acid methyl esters (FAME) with unsaturated bonds (C=C), polymer and biodiesel may co-oxidize on direct contact. The reactions may be more active if the polymers also contain unsaturated carbon bonds. The rate of interaction depends on the sensitivity of the polymer to several influencing factors, including the composition of the polymer itself.

In our experiments, weight increase of both Capron 8202 and 8351 specimens clearly indicates that all three fuels were absorbed into the polymers. Tensile tests

have shown that both yield and tensile strengths decreased after immersion in all three fuels. The DMA experiments have shown that there were significant decreases in the glass transition temperature and storage modulus. Peak $\tan \delta$ and loss modulus, on the other hand, increased. There was also a broadening of the $\tan \delta$ peak. DSC measurements indicated that there was a modest increase in crystallinity; however, the melting peak was not much affected. Finally, FTIR absorbance data indicated that the IR peaks did not shift and no new peaks appeared after immersion. Since there were no new peaks and all the peaks that were observed with unimmersed polymers also appeared in immersed polymers, it is concluded that no chemical changes occurred due to the absorption of any of the fuels.

Decrease in T_g and broadening of $\tan \delta$ peaks after immersion indicate that the absorbed fuels are acting like a plasticizer. The small hydrocarbon molecules of diesel and fatty acid molecules of biodiesel diffuse between the polyamide molecules, thus reducing the strength of secondary bonding between them. Plasticizing effect is also evident when storage moduli of unimmersed and immersed polymers are compared. Reductions in yield and tensile strengths, although not as large as those of storage moduli, are also due to the plasticizing effect.

Rios de Andes et al. [26] observed decreases in glass transition temperature of polyamide-6,6 after immersion in a series of polar, amphiphilic and non-polar solvents. They attributed the decrease in glass transition temperature to alteration of molecular mobility due to breakage of interchain hydrogen bonds in the case of polar solvents and modification of hydrogen bonds through steric effects in the case of non-polar solvents. Sfirakis and Rogers [27] conducted immersion experiments with polyamide-6 in water, methanol and ethanol, and observed that crystallinity of

polyamide-6 was not appreciably affected by the absorption of these three fluids. The properties of polyamide-6 were reduced by their diffusion into the polymer. They concluded that the absorption mainly took place in the amorphous region and the mobility of the polymer molecules was reduced by their presence. Laurati et al. [28] observed that absorption of water and ethanol molecules in semi-crystalline aromatic and aliphatic polyamide-6,6 induced some reorganization of the hydrogen bonds in the crystalline phase, but also increased the mobility of the amorphous segments of the molecules in the interlamellar regions. Similar observations are summarized by Murthy [29] in his review article which addressed the effect of solvents on aliphatic polyamides, such as polyamide-6.

In the current study, the crystallinity was modestly affected by the absorption of all three fuels into both Capron 8202 and 8351. The molecules of both diesel and biodiesel were perhaps also absorbed in the amorphous region, but their absorption has created a plasticizing effect which resulted in lowering of the glass transition temperature, storage modulus and strengths. Since the liquids used in this study are non-polar, the plasticization effect may be attributed to the steric effects as suggested in Ref. [26].

5. CONCLUSIONS

This study investigated the effect of biodiesel on two polyamide-6 based semi-crystalline polymers, a homopolymer (Capron 8202) and a graft copolymer (Capron 8351) using immersion tests at 25°C. In addition to biodiesel, the effects of diesel and a 20/80 blend of diesel and biodiesel were also considered. Immersion of both polymers in all three fuels caused increase in weight due to absorption of fuels; however, the weight increase did not reach the equilibrium level in 720 hours. The

weight increase was the highest in biodiesel and lowest in diesel under both stressed and unstressed conditions. Both yield and tensile strengths of Capron 8202 and 8351 decreased after immersion in all three fuels; however, the tensile failure mode remained ductile. The glass transition temperature, storage modulus and peak $\tan \delta$ decreased and the loss modulus increased. The degree of crystallinity increased slightly, while the melting peak was not influenced much. No changes in the chemical structure was observed in the FTIR data.

Based on the experimental observations reported here, it is concluded that all three fuels acted as plasticizers in both polyamide-6 based semi-crystalline polymers investigated in this research, and it appears that there were no chemical degradation for up to 720 hours of exposure at room temperature. In terms of aggressivity among the three fuels considered, the effect of biodiesel absorption appears to be slightly higher than diesel in both polymers.

REFERENCES

- [1] Richaud E, Djouani F, Fayyolle B, Verdu J and Flaconnèche B. “New insights in polymer-biofuels interaction”, *Oil & Gas Sci. and Tech.*, 2015, 70: 317-333.
- [2] Hoekman S K, Broch A, Robbins C, Cenicerros, E and Natarajan, M, “Review of biodiesel composition, properties, and specifications”, *Renewable and Sustainable Energy Reviews*, 2012, 16(1): 143-169.
- [3] Basha S A, Gopal K R and Jebaraj S., “A review on biodiesel production, combustion, emissions and performance”, *Renewable and Sustainable Energy Reviews*, 2009, 13(6): 1628-1634.
- [4] Pinzi S, Garcia I L, Lopez-Gimenez F J, Luque de Castro M D, Dorado G and

Dorado M P, “The ideal vegetable oil-based biodiesel composition: a review of social, economical and technical implications”, *Energy & Fuels*, 2009, 23(5): 2325-2341.

- [5] Atabani A E, Silitonga A S, Badruddin I A, Mahlia T M I, Masjuki H H and Mekhilef S, “A comprehensive review on biodiesel as an alternative energy resource and its characteristics”, *Renewable and Sustainable Energy Reviews*, 2012, 16(4): 2070-2093.
- [6] Haseeb A, Fazal M A, Jahirul M I and Masjuki H H. “Compatibility of automotive materials in biodiesel: a review”, *Fuel*, 2011, 90(3): 922-931.
- [7] Besse, G B and Fey, J P, “Compatibility of elastomers and metals in biodiesel fuel blends”, SAE 971690, 1997.
- [8] Haseeb A S M A, Masjuki H H, Siang C T and Fazal M A, “Compatibilty of elastomers in palm biodiesel”, *Renewable Energy*, 2010, 35: 2356-2361.
- [9] Haseeb A S M A, Jun T S, Fazal M A and Masjuki H H, “Degradation of physical properties of different elastomers upon exposure to palm biodiesel”, *Energy*, 2012, 36: 1814-1819.
- [10] Alves S M, Mello V S and Medeiros J S, “Palm and soybean biodiesel compatibility with fuel system elastomers”, *Tribology International*, 2013, 65:74-80.
- [11] Terry B, McCormick R L and Natarajan M, “Impact of biodiesel blends on fuel system component durability”, SAE 2006-01-3279, 2006.
- [12] Thomas E W, Fuller R E and Terauchi K, “Fluoroelastomer compatibility with biodiesel fuels”, SAE 2007-01-4061, 2007.

- [13] Nakai T and Ogishi H, “Verification of influences of biodiesel fuel on automotive fuel-line rubber and plastic materials”, SAE 2010-01-0915, 2010.
- [14] Richaud E, Flaconnèche B, Verdu J. “Biodiesel permeability in polyethylene”, *Polymer Testing*, 2012, 31(8): 1070-1076.
- [15] Böhning M, Niebergall U, Adam A and Stark W, “Impact of biodiesel sorption on mechanical properties of polyethylene”, *Polymer Testing*, 2014, 34:17-24.
- [16] Böhning M, Niebergall U, Adam A and Stark W, “Influence of biodiesel sorption on temperature-dependent impact properties of polyethylene”, *Polymer Testing*, 2014, 40:133-142.
- [17] Böhning M, Niebergall U, Zanotto M and Wachtendorf V, “Impact of biodiesel sorption on tensile properties of PE-HD for container applications”, *Polymer Testing*, 2016, 50:315-324.
- [18] Lutz G and Mata-Segreda J F, “Kinetics of interaction of palm ethyl biodiesel with three different polymer materials”, *J. Physical Organic Chemistry*, 2008, 21:1068-1071.
- [19] Ullah K, “Aging of polymer in diesel and biodiesel blended fuel”, Master’s Thesis, Chalmers University of Technology, Goteborg, Sweden, 2013.
- [20] Boleno B, Benjamin E, Desai K, Norfolk L and Carvalho A, “Design considerations for high-performance polymers used in biofuel components”, SAE 2011-36-0021, 2011.
- [21] Gomej-Mares M, Martinez-Ortega M E, Arroyo-Ortega G, Reyes-Blas H, Hernandez-Paz J and Marquez-Marquez C. “Comparative study of the effects of diesel and biodiesel over POM, PPA and PPS polymers used in automotive

industry”, *J. Materials Sciences and Engineering*, 2014, 3:142.
doi:10.4172/2169-0022.1000142.

[22] Baena L M, Zuleta E C and Calderón, J A, “Evaluation of the stability of polymeric materials exposed to palm biodiesel and biodiesel-organic acid blends”, *Polymers*, 2018, 10:511-528.

[23] <http://www.matweb.com/search/datasheetText.aspx?bassnum=PALC21>, BASF Capron 8202 Nylon-6

[24] <http://www.matweb.com/search/datasheettext.aspx?matguid=8b59b3a432504220ae283074405b309f>, BASF Capron 8351 impact modified Nylon-6.

[25] Birley A W, Haworth B and Batchelor J. *Physics of Plastics*. Hanser Publishers, Munich, Germany, 1991.

[26] Rios de Anda A, Fillot L A, Rossi S, Long D and Sotta P. “Influence of the sorption of polar and non-polar solvent on the glass transition temperature of polyamide 6,6 amorphous phase”, 2011, *Polymer Eng. Sci*, 51:2129-2135.

[27] Sfirakis A and Rogers C E. “Effects of sorption modes on the transport and physical properties of nylon 6”, *Polymer Eng. Sci.*, 1980, 20(4): 294-299.

[28] Laurati M, Arbe A, Rios de Anda A, Fillot L A and Sotta P. “Effect of polar solvents on the crystalline phase of polyamides”, *Polymer*, 2014, 55: 2867-2881.

[29] Murthy N S. “Hydrogen bonding, mobility, and structural transitions in aliphatic polyamides”, *J. Polymer Sci., Part B: Polymer Physics*, 2006, 44:1763-1782.

LIST OF TABLES

- Table 1: Weight increase after 720 hours of immersion at 25°C
- Table 2: Yield and tensile strengths of Capron 8202 and 8351 before and after 720-hr. immersion at 25°C⁽¹⁾
- Table 3: T_g , peak $\tan \delta$, storage modulus and loss modulus of Capron 8202 and 8351 before and after 720-hr. immersion at 25°C
- Table 4: Degree of crystallinity and melting temperature of Capron 8202 and 8351 before and after 720-hr. immersion at 25°C
- Table 5: FTIR wave numbers observed for Capron 8202 and 8351 before and after 720-hr. immersion at 25°C⁽¹⁾

LIST OF FIGURES

- Figure 1: Typical biodiesel and diesel molecules
- Figure 2: Specimen inserted in a C-channel and the assumed specimen geometry in stressed immersion test
- Figure 3: Percentage weight increase of Capron 8202 in diesel, B20 and B100 as a function of time
- Figure 4: Percentage weight increase of Capron 8351 in diesel, B20 and B100 as a function of time
- Figure 5: Tensile failure modes of specimens before and after immersion: (a) Capron 8202 before immersion, (b) Capron 8351 before immersion, (c) Capron 8202 after 720-hours immersion in B100, (d) Capron 8351 after 720-hours immersion in B100
- Figure 6: DMA diagrams of (a) Capron 8202 and (b) Capron 8351, both before immersion
- Figure 7: Variation of glass transition temperatures of Capron 8202 and 8351 with immersion time
- Figure 8: Variation of peak $\tan \delta$ of Capron 8202 and 8351 with immersion time
- Figure 9: $\tan \delta$ of Capron 8202 as a function of temperature before and after immersion in B100 (top), B20 (middle) and diesel (bottom) for 720 hours
- Figure 10: Variation of storage moduli of Capron 8202 and 8351 with immersion time
- Figure 11: Variation of loss moduli of Capron 8202 and 8351 with immersion time

Figure 12: DSC thermograms of Capron 8202 and 8351 specimens before and after immersion in B100 for 720 hours: (a) Capron 8202 before immersion, (b) Capron 8351 before immersion, (c) Capron 8202 after immersion, (d) Capron 8351 after immersion

Figure 13: Variation of degree of crystallinity of Capron 8202 and 8351 as a function of immersion time

Figure 14: FTIR absorbance spectra of Capron 8202 and 8351 before immersion and after 720-hour immersion

Table 1: Weight increase after 720 hours of immersion at 25°C

Fuel	Percentage Weight Increase after 720 Hours of Immersion ⁽¹⁾			
	Unstressed		Stressed	
	8202	8351	8202	8351
Diesel	1.439	1.377	1.560	1.312
B20	1.756	1.560	1.866	1.511
B100	2.041	1.643	2.231	1.753

(1) Average of 5 specimens for each condition

Table 2: Yield and tensile strengths of Capron 8202 and 8351 before and after 720-hr. immersion at 25°C⁽¹⁾

Immersion Condition		Capron 8202		Capron 8351	
		Yield Strength (MPa)	Tensile Strength (MPa)	Yield Strength (MPa)	Tensile Strength (MPa)
Before immersion		62.7	67.3	40.7	44.2
After 720-hr. immersion @ 25 °C	DIESEL	59.7	64.5	38.6	42.5
	B20	58.2	65.1	36.4	37.8
	B100	58.4	64.5	38.5	43.1
After 720-hr. stressed immersion @25°C	DIESEL	56.0	64.7	34.8	37.7
	B20	54.5	63.3	32.7	37.4
	B100	51.5	61.0	34.0	39.1

(1) Average of 3 specimens for each condition

Table 3: T_g , peak $\tan \delta$, storage modulus and loss modulus of Capron 8202 and 8351 at 25°C

Material	Time of Immersion (Hour)	Condition		T_g (°C)	Peak $\tan \delta$	Storage modulus (GPa)	Loss Modulus (MPa)
Capron 8202	0	Dry		70.77	0.1254	1.835	0.0466
	After Immersion						
	720	25°C	Diesel	53.10	0.1049	1.372	113.400
	720	25°C	B20	46.65	0.1038	1.188	116.800
	720	25°C	B100	32.90	0.1029	1.239	121.500
	720 (Stressed)	25°C	Diesel	45.30	0.1142	1.377	130.460
			B20	32.05	0.1067	1.197	124.350
B100			30.55	0.1099	1.078	116.540	
Capron 8351	0	Dry		70.2	0.1303	1.314	0.0619
	After Immersion						
	720	25°C	Diesel	56.40	0.1176	1.134	92.500
	720	25°C	B20	57.35	0.1078	1.168	94.860
	720	25°C	B100	56.10	0.1078	1.215	92.100
	720 (Stressed)	25°C	Diesel	55.25	0.1235	0.967	91.703
			B20	56.15	0.1120	0.868	88.673
B100			56.25	0.1102	0.773	78.912	

Table 4: Degree of crystallinity and melting temperature of Capron 8202 and 8351 before and after 720-hr. immersion at 25°C

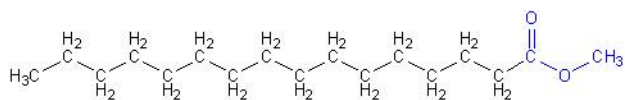
Immersion Time (Hour)	Immersion Condition		Capron 8202		Capron 8351	
			% Crystallinity	T _m (°C)	% Crystallinity	T _m (°C)
0	Before Immersion		29.23	223.61	19.57	221.63
720	25°C	Diesel	31.5	225.99	19.93	221.02
720	25°C	B20	36.17	223.98	18.99	221.28
720	25°C	B100	33.49	224.49	24.47	221.64
720 (Stressed)	25°C	Diesel	31.13	224.12	20.28	221.64
		B20	30.38	224.42	20.03	222.48
		B100	33.85	223.97	19.01	220.06

Table 5: FTIR wave numbers observed for Capron 8202 and 8351 before and after 720-hr. immersion at 25°C ⁽¹⁾

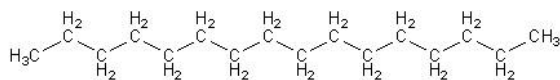
Standard Wave Numbers (cm ⁻¹)	Functional Group	Capron 8202				Capron 8351			
		Before Immersion	Diesel	B20	B100	Before Immersion	Diesel	B20	B100
3294	N-H stretching	3294	3302	3295	3294	3300	3295	3300	3300
3083	N-H stretching	3084	3083	3089	3094	3082	3085	3085	3085
2937	Antisymmetric CH ₂ stretching	2924	2932	2924	2922	2918	2919	2918	2918
2868	Symmetric CH ₂ stretching	2860	2859	2856	2857	2850	2850	2850	2850
1645	C=O stretching	1635	1635	1635	1635	1635	1635	1635	1635
1545	C-N stretching	1536	1536	1536	1536	1537	1541	1541	1541
1477	CH ₂ scissor vibration	1462	1460	1460	1460	1460	1460	1460	1461
1417	CH ₂ scissor vibration	1432	1417	1417	1417	1417	1417	1417	1417
1374	CH ₂ wagging vibration	1370	1370	1370	1370	1370	1374	1374	1370
1264	N-H bending & C-N stretching	1262	1262	1262	1262	1262	1262	1262	1262

1201	CH ₂ twist-wagging vibration	1202	1201	1202	1202	1202	1202	1202	1202
1170	CO-NH skeletal motion	1168	1168	1168	1168	1168	1168	1168	1168
960	C=O & N-H in-plane vibration	975	975	975	975	975	975	975	975
692	NH out-of-plane bending	690	688	688	688	686	685	685	686

(1) Immersion time 720 hours at 25°C



Typical biodiesel molecule



Typical diesel molecule

Figure 1: Typical biodiesel and diesel molecules

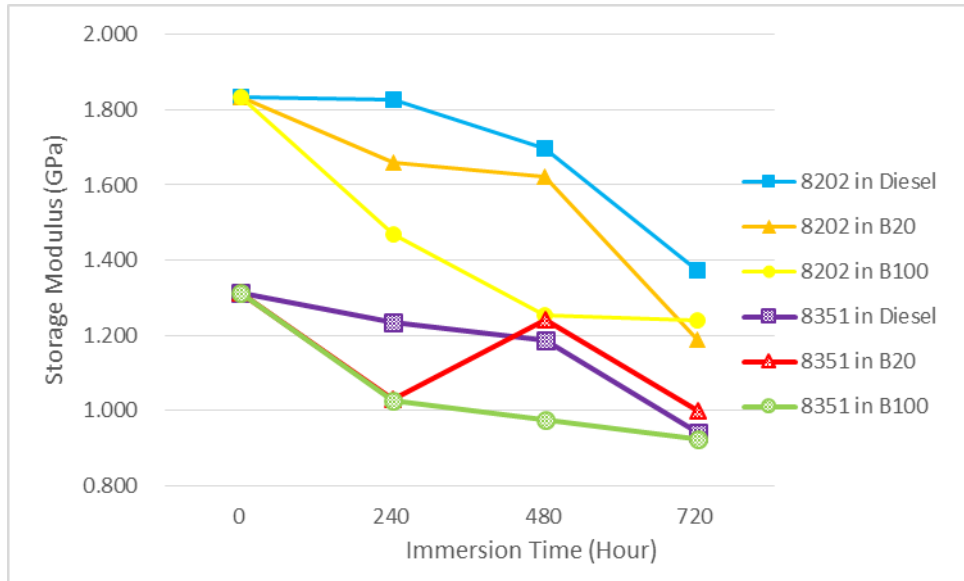


Figure 10: Variation of storage moduli of Capron 8202 and 8351 with immersion time

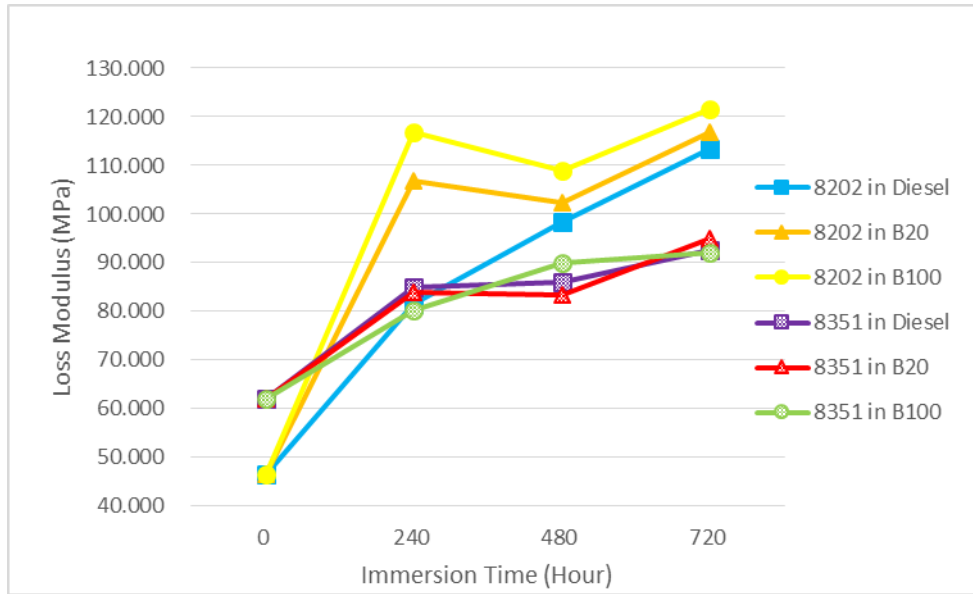


Figure 11: Variation of loss moduli of Capron 8202 and 8351 with immersion time

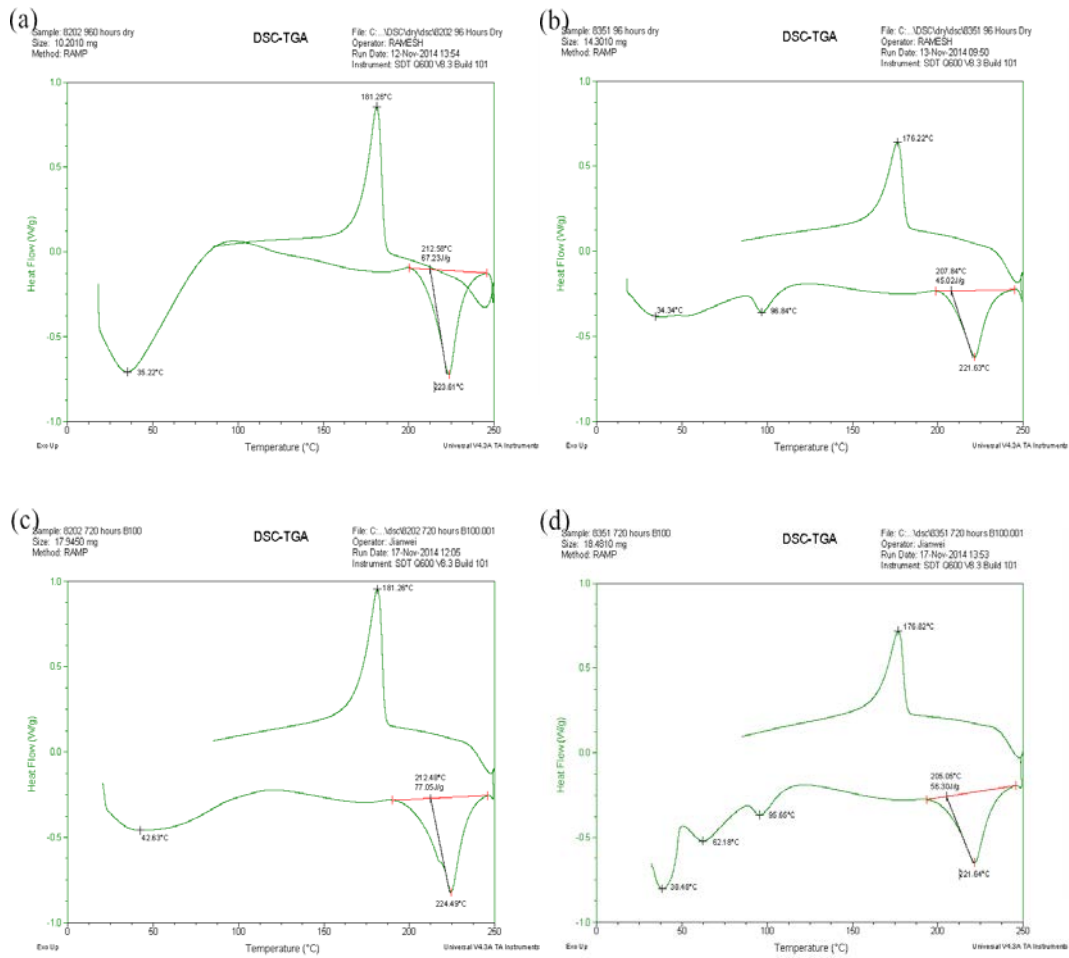


Figure 12: DSC thermograms of Capron 8202 and 8351 specimens before and after immersion in B100 for 720 hours: (a) Capron 8202 before immersion, (b) Capron 8351 before immersion, (c) Capron 8202 after immersion, (d) Capron 8351 after immersion

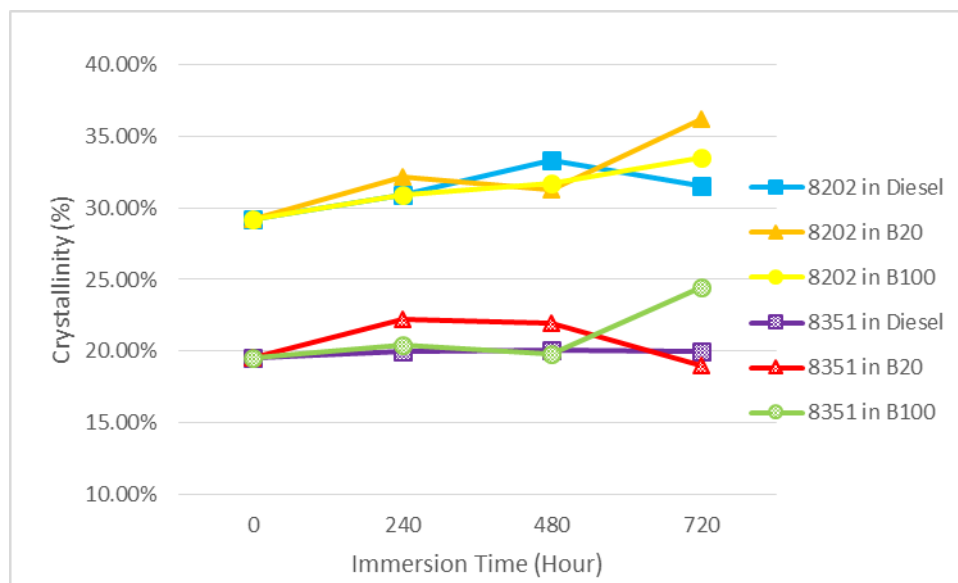
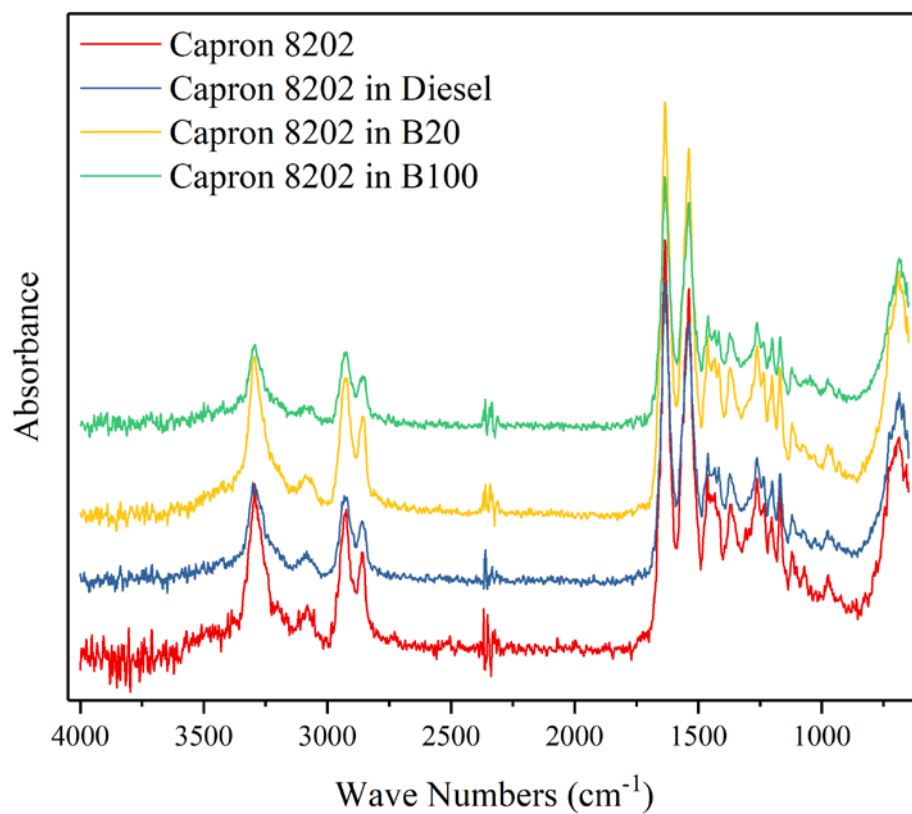


Figure 13: Variation of degree of crystallinity of Capron 8202 and 8351 as a function of immersion time



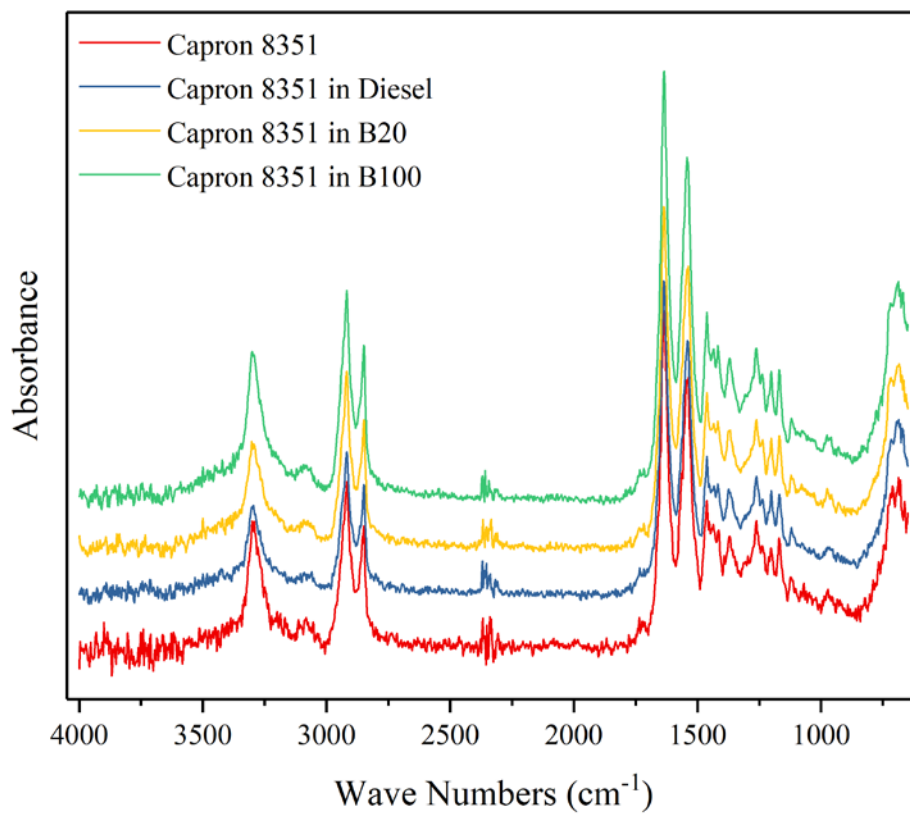


Figure 14: FTIR absorbance spectra of Capron 8202 and 8351 before immersion and after 720-hour immersion

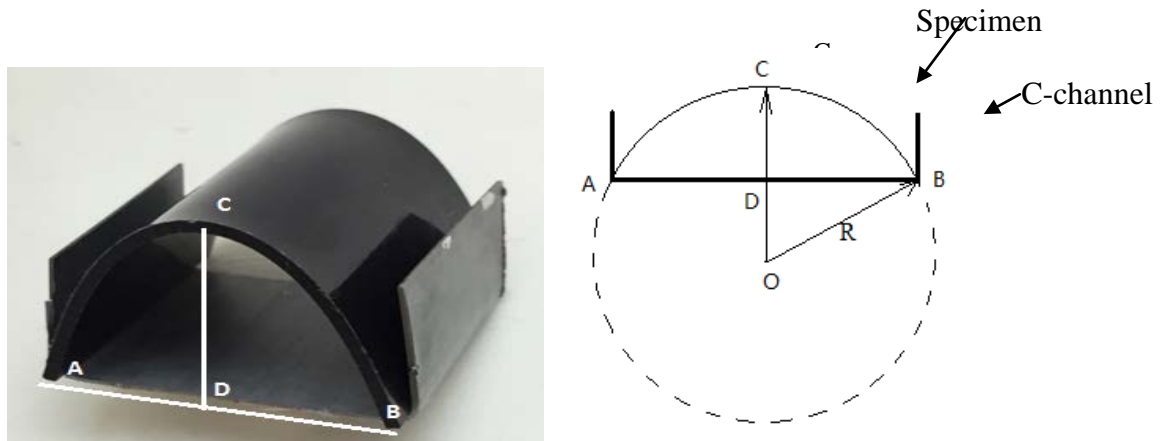


Figure 2: Specimen inserted in a C-channel and the assumed specimen geometry in stressed immersion test

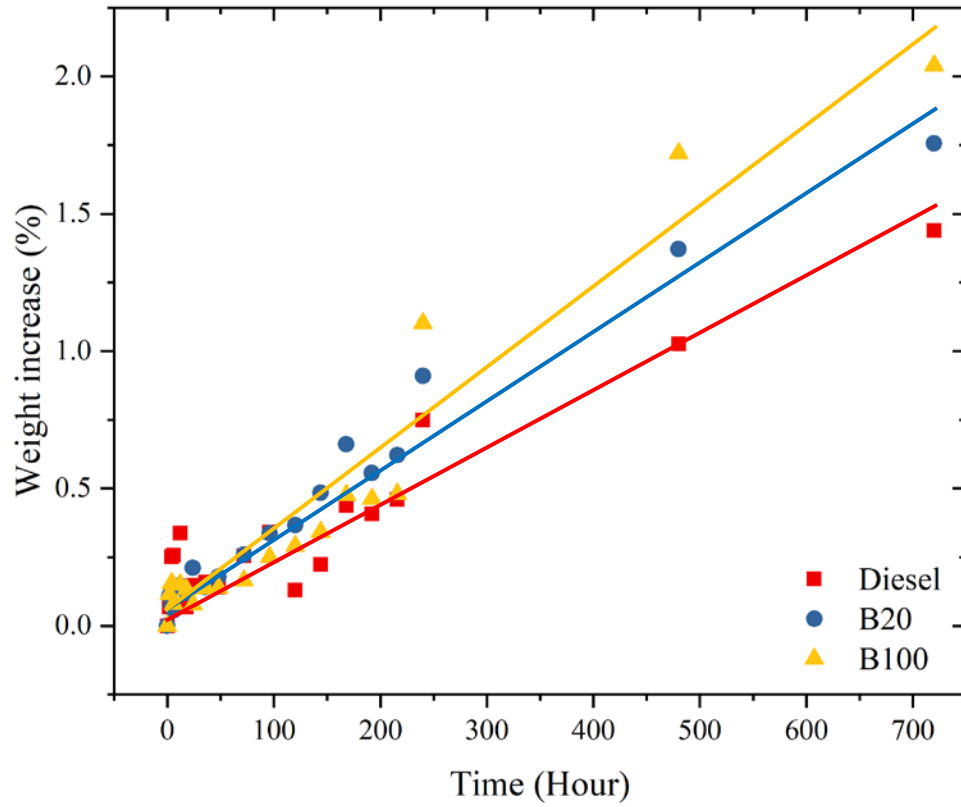


Figure 3: Percentage weight increase of Capron 8202 in diesel, B20 and B100 as a function of time

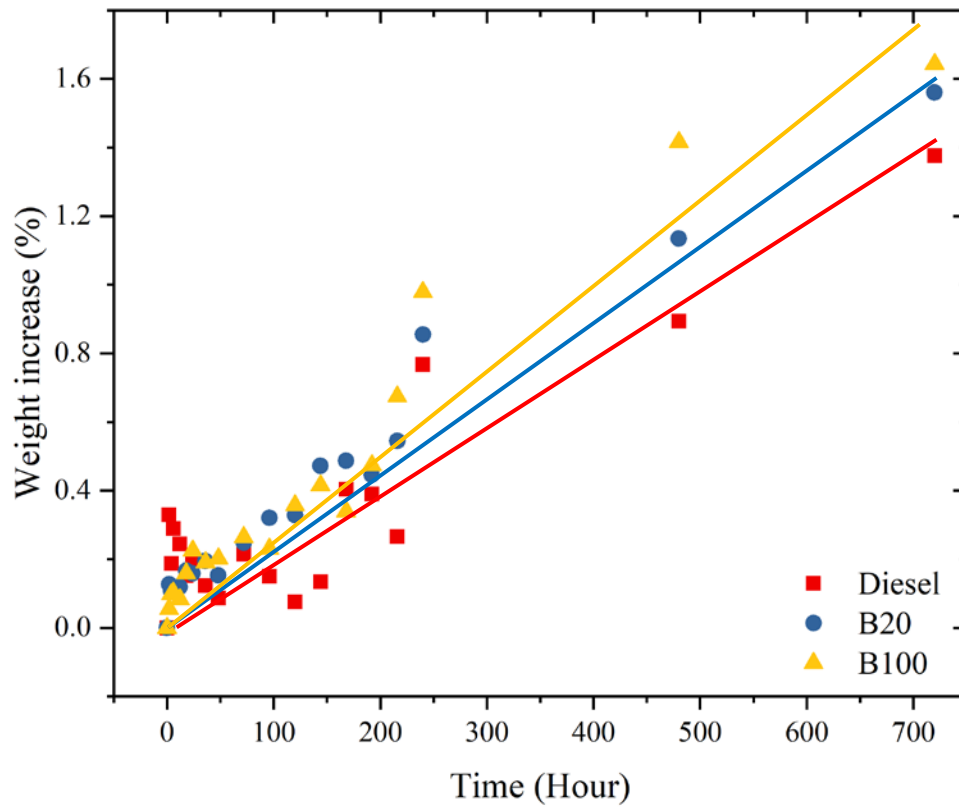


Figure 4: Percentage weight increase of Capron 8351 in diesel, B20 and B100 as a function of time

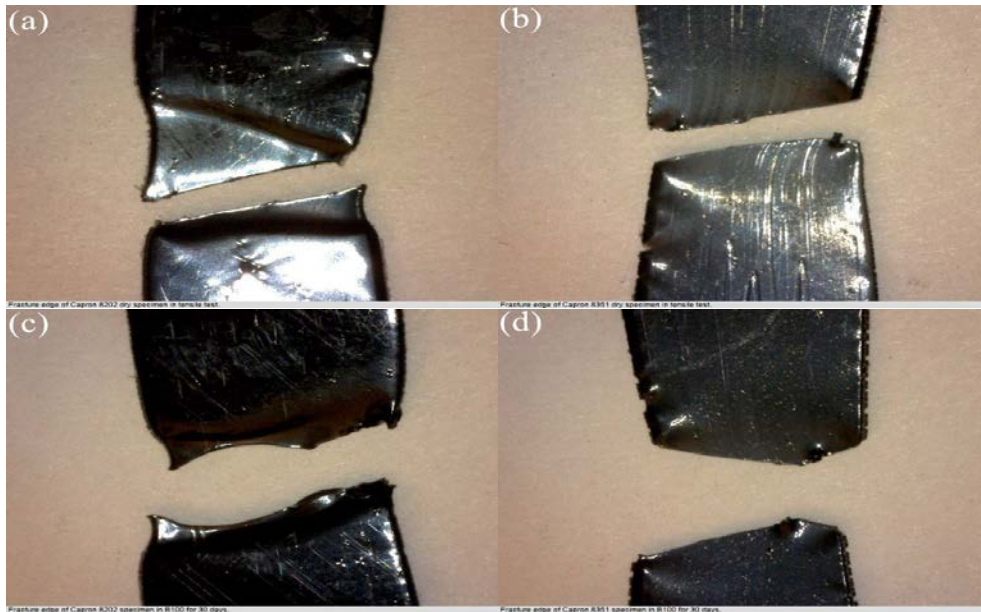
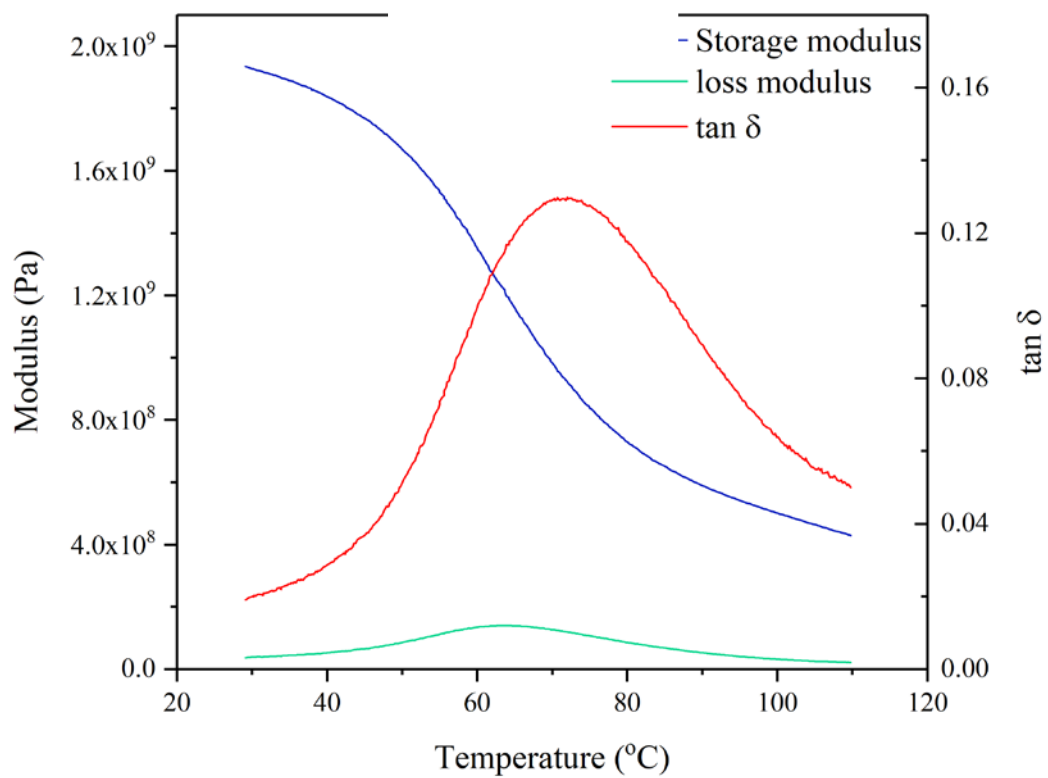


Figure 5: Tensile failure modes of specimens before and after immersion: (a) Capron 8202 before immersion, (b) Capron 8351 before immersion, (c) Capron 8202 after 720-hours immersion in B100, (d) Capron 8351 after 720-hours immersion in B100



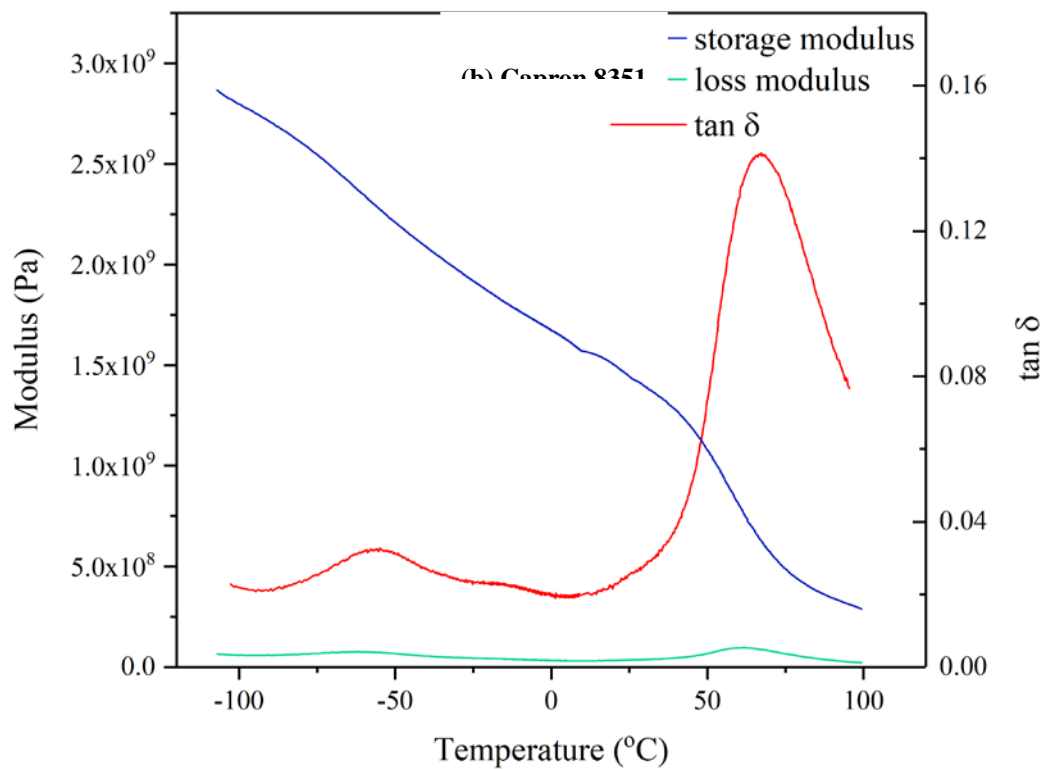


Figure 6: DMA diagrams of (a) Capron 8202 and (b) Capron 8351, both before immersion

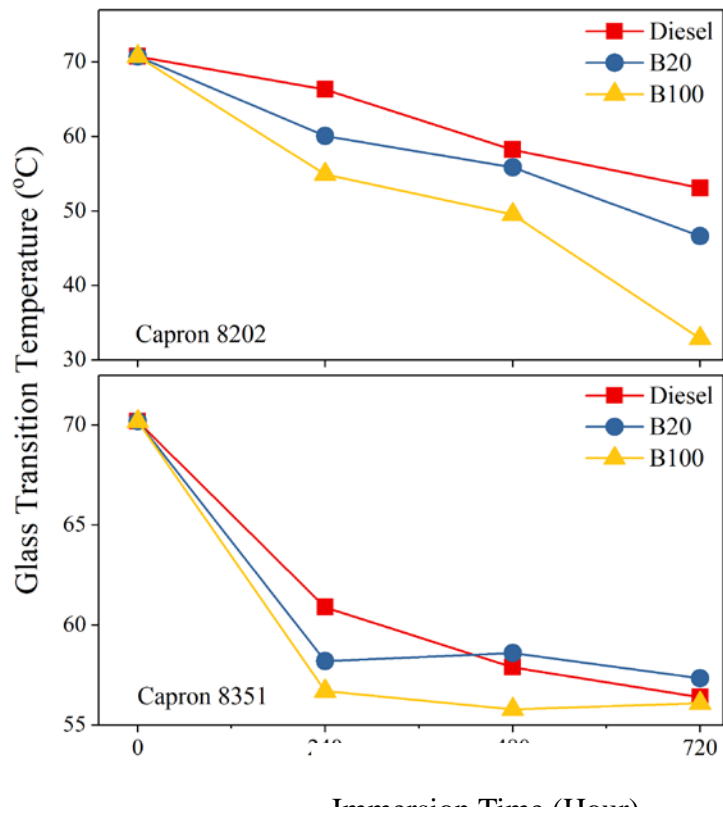


Figure 7: Variation of glass transition temperatures of Capron 8202 and 8351 with immersion time

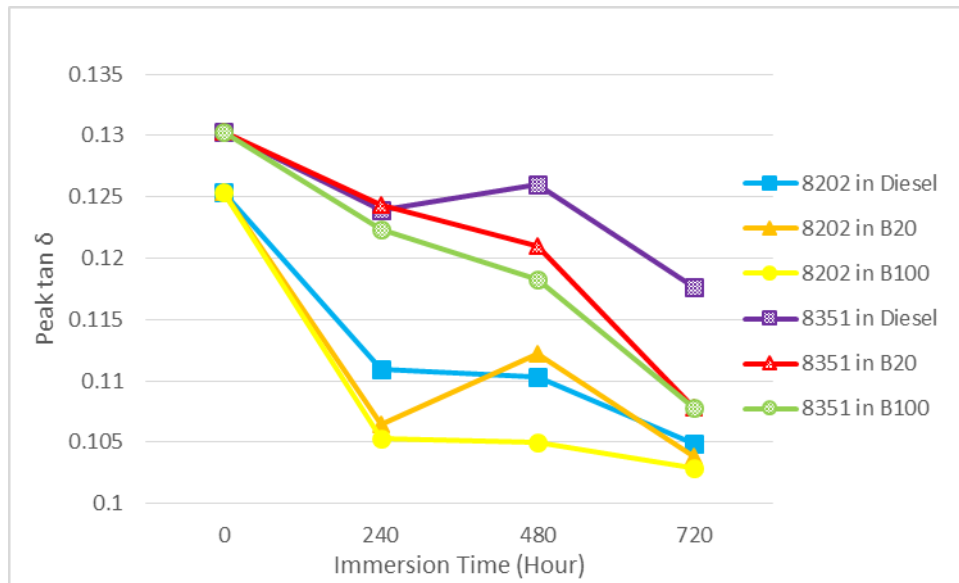
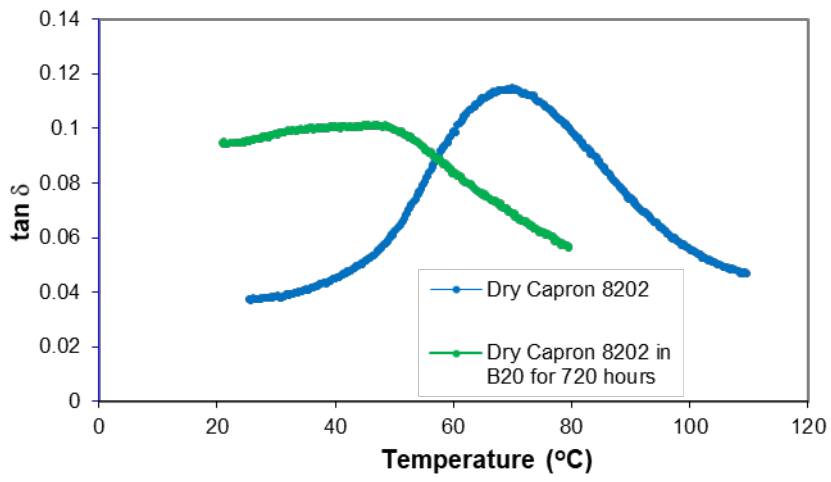
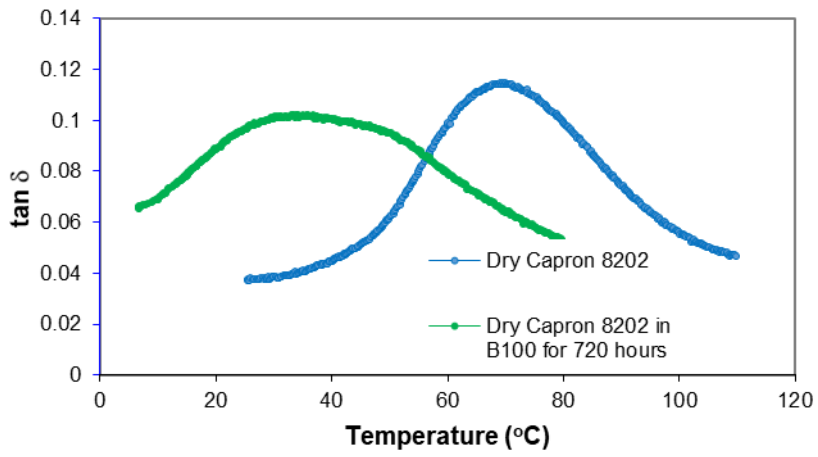


Figure 8: Variation of peak $\tan \delta$ of Capron 8202 and 8351 with immersion time



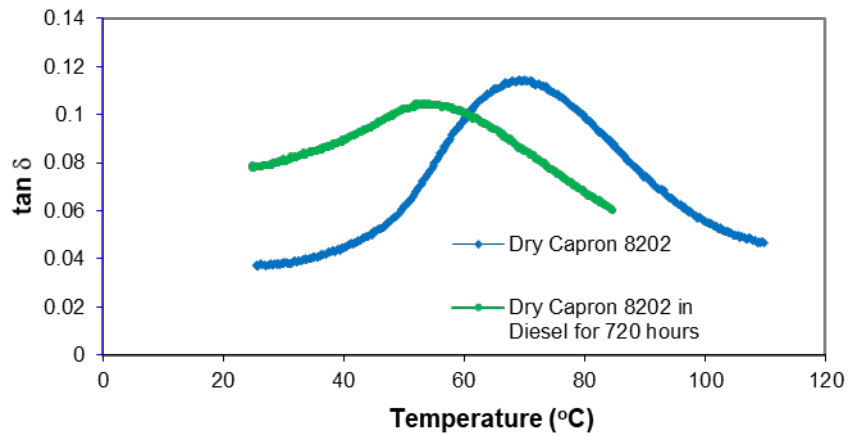
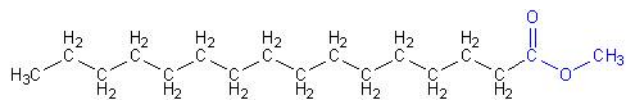
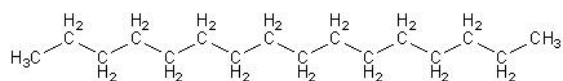


Figure 9: $\tan \delta$ of Capron 8202 as a function of temperature before and after immersion in B100 (top), B20 (middle) and diesel (bottom) for 720 hours



Typical biodiesel molecule



Typical diesel molecule

Figure 1: Typical biodiesel and diesel molecules

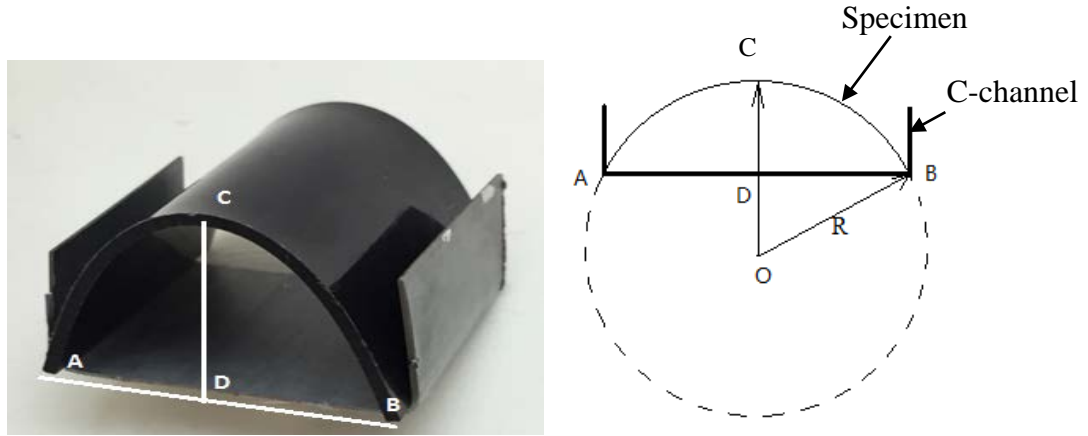


Figure 2: Specimen inserted in a C-channel and the assumed specimen geometry in stressed immersion test

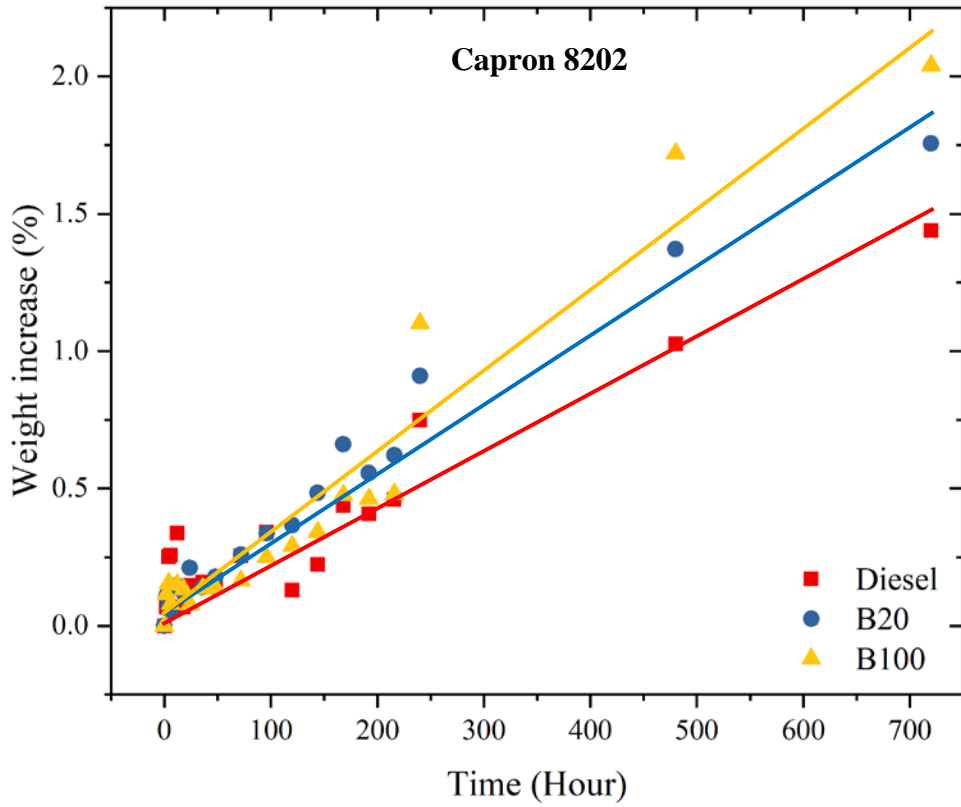


Figure 3: Percentage weight increase of Capron 8202 in diesel, B20 and B100 as a function of time

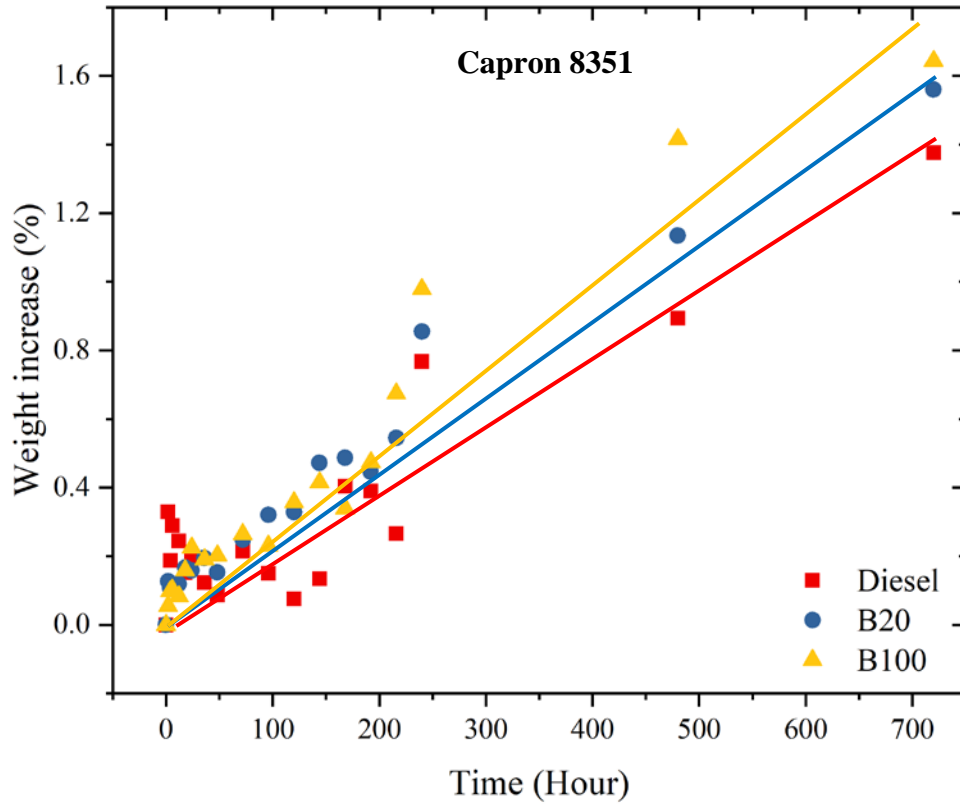


Figure 4: Percentage weight increase of Capron 8351 in diesel, B20 and B100 as a function of time

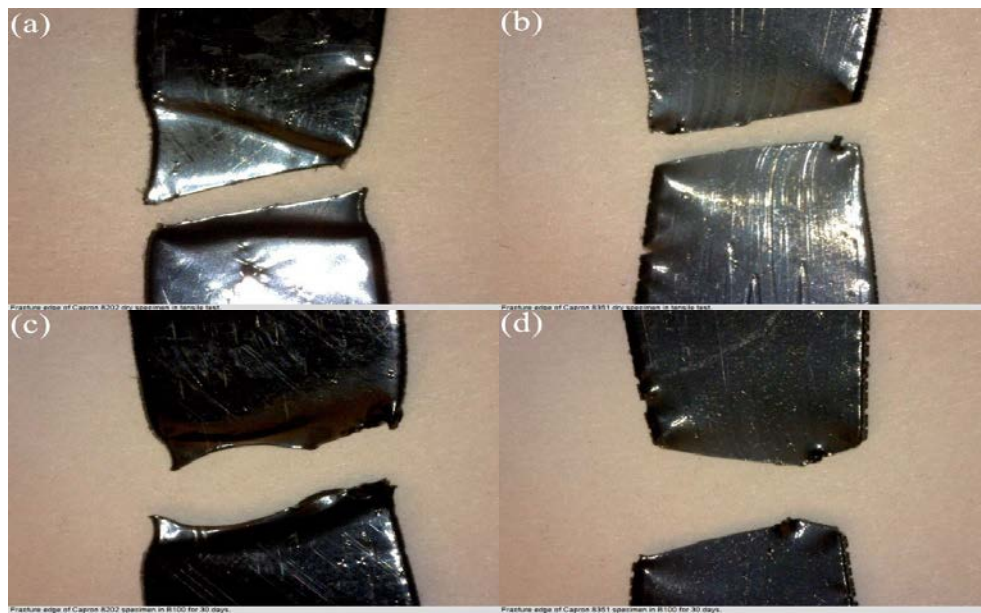


Figure 5: Tensile failure modes of specimens before and after immersion: (a) Capron 8202 before immersion, (b) Capron 8351 before immersion, (c) Capron 8202 after 720-hours immersion in B100, (d) Capron 8351 after 720-hours immersion in B100

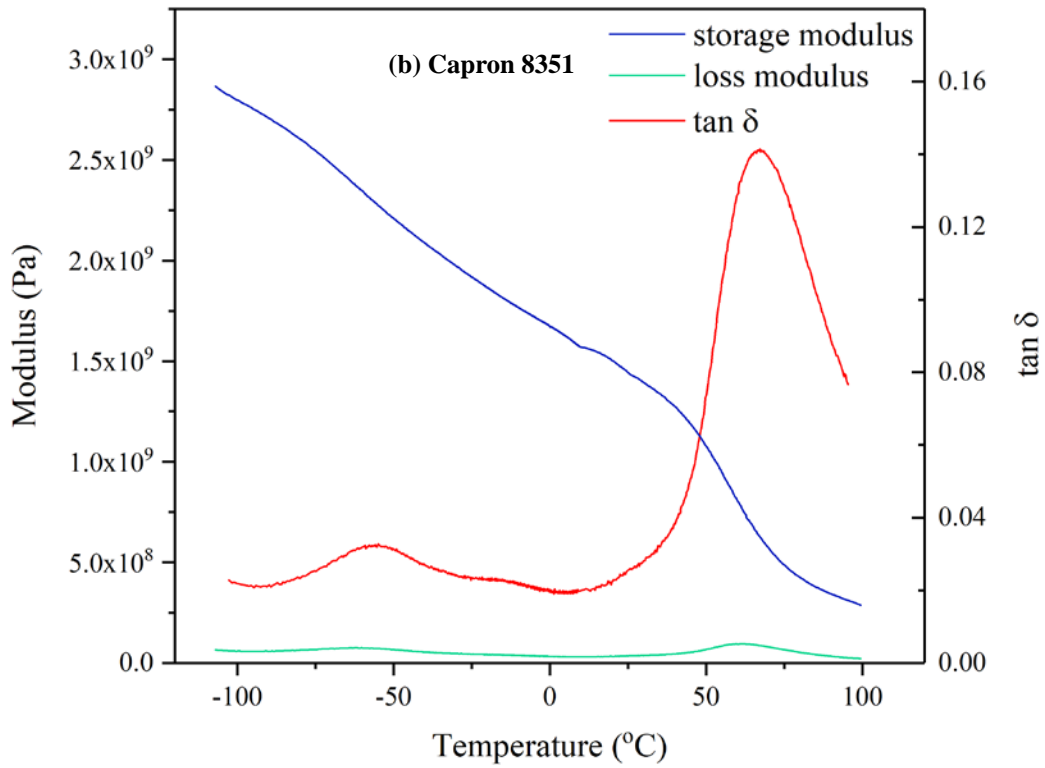
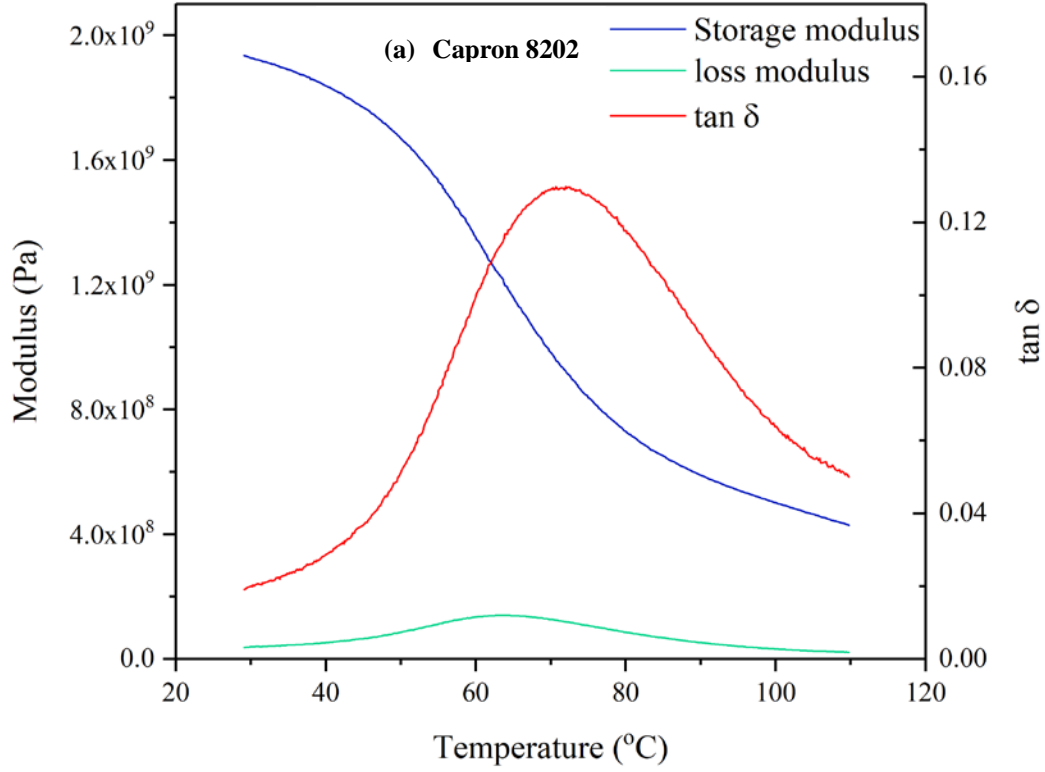


Figure 6: DMA diagrams of (a) Capron 8202 and (b) Capron 8351, both before immersion

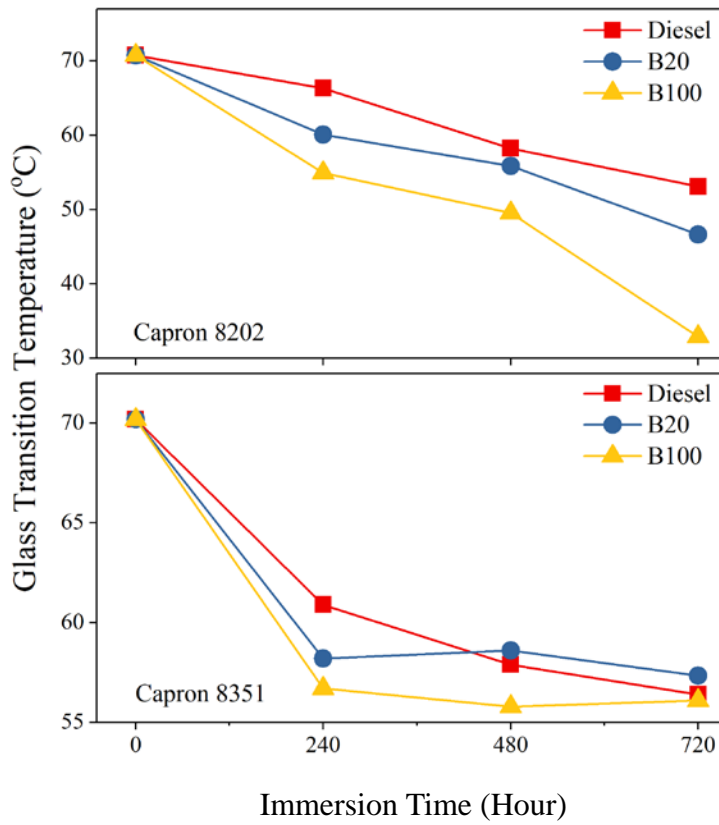


Figure 7: Variation of glass transition temperatures of Capron 8202 and 8351 with immersion time

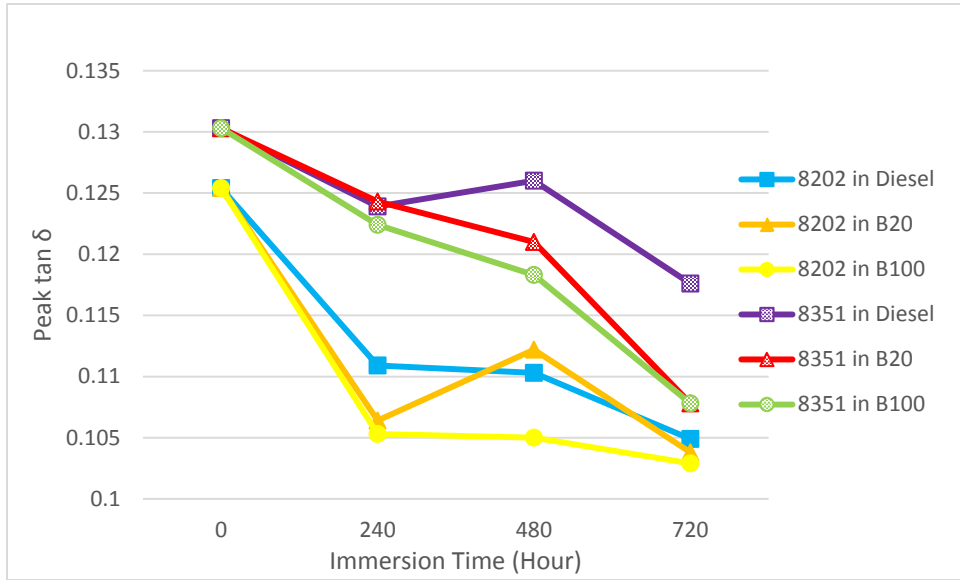


Figure 8: Variation of peak $\tan \delta$ of Capron 8202 and 8351 with immersion time

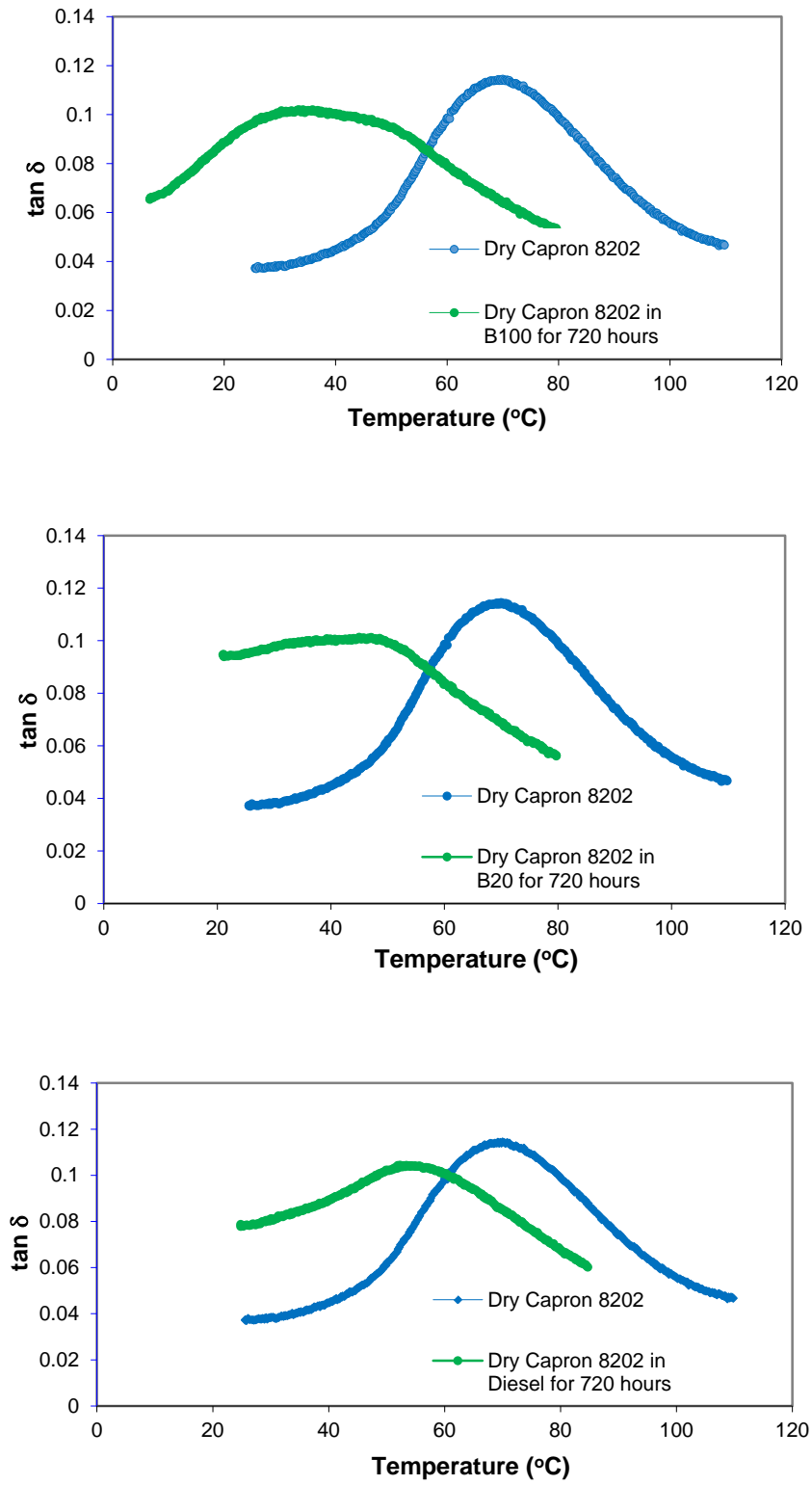


Figure 9: $\tan \delta$ of Capron 8202 as a function of temperature before and after immersion in B100 (top), B20 (middle) and diesel (bottom) for 720 hours

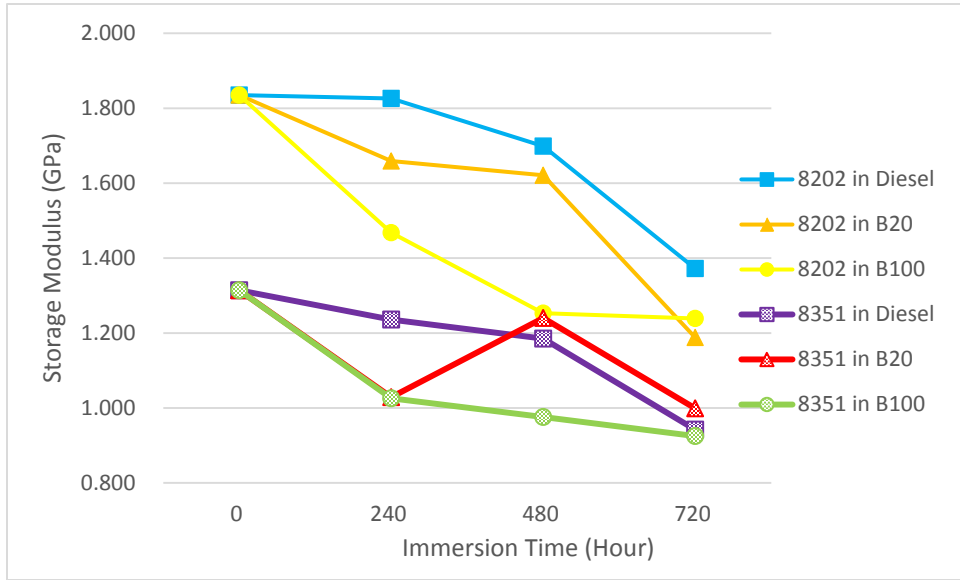


Figure 10: Variation of storage moduli of Capron 8202 and 8351 with immersion time

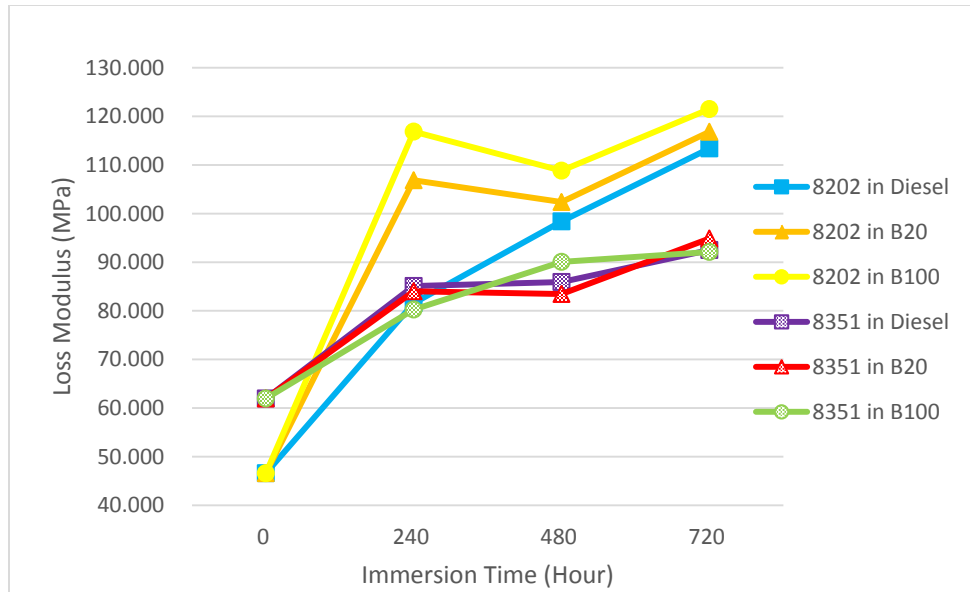


Figure 11: Variation of loss moduli of Capron 8202 and 8351 with immersion time

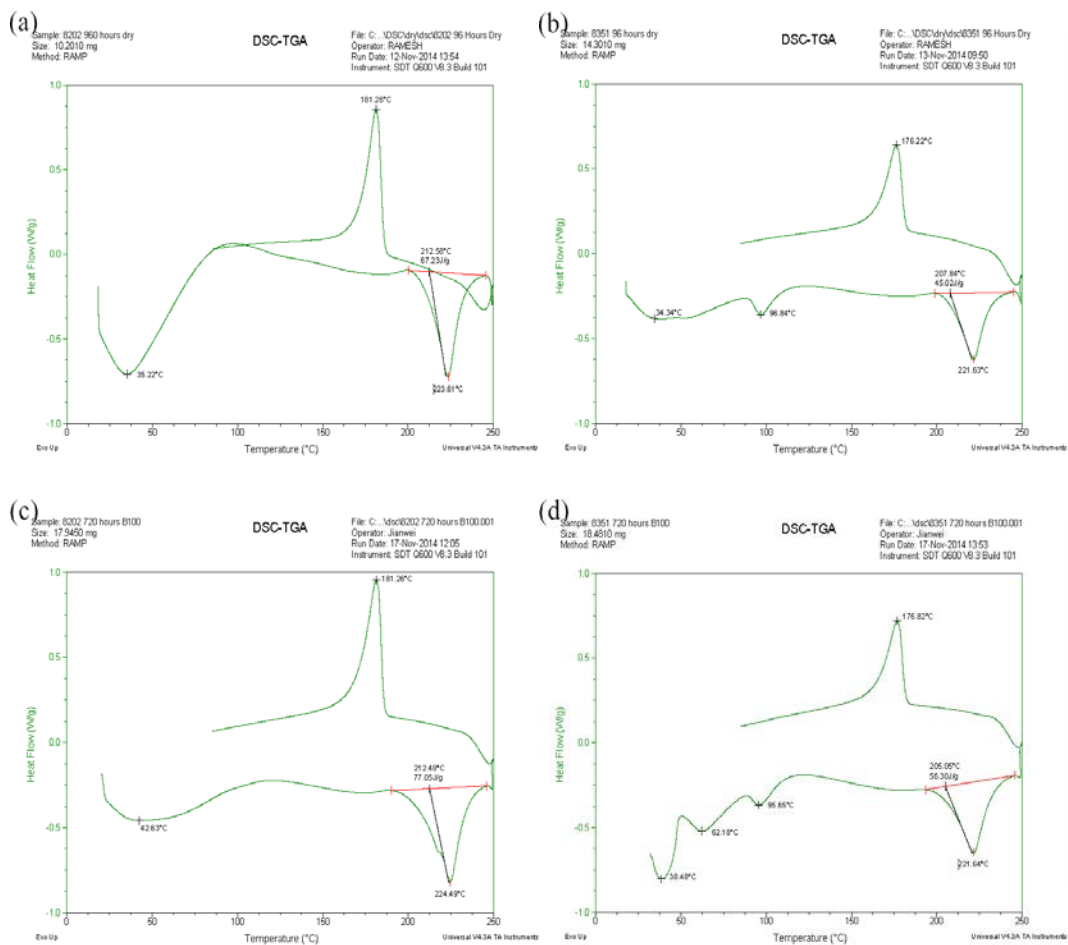


Figure 12: DSC thermograms of Capron 8202 and 8351 specimens before and after immersion in B100 for 720 hours: (a) Capron 8202 before immersion, (b) Capron 8351 before immersion, (c) Capron 8202 after immersion, (d) Capron 8351 after immersion

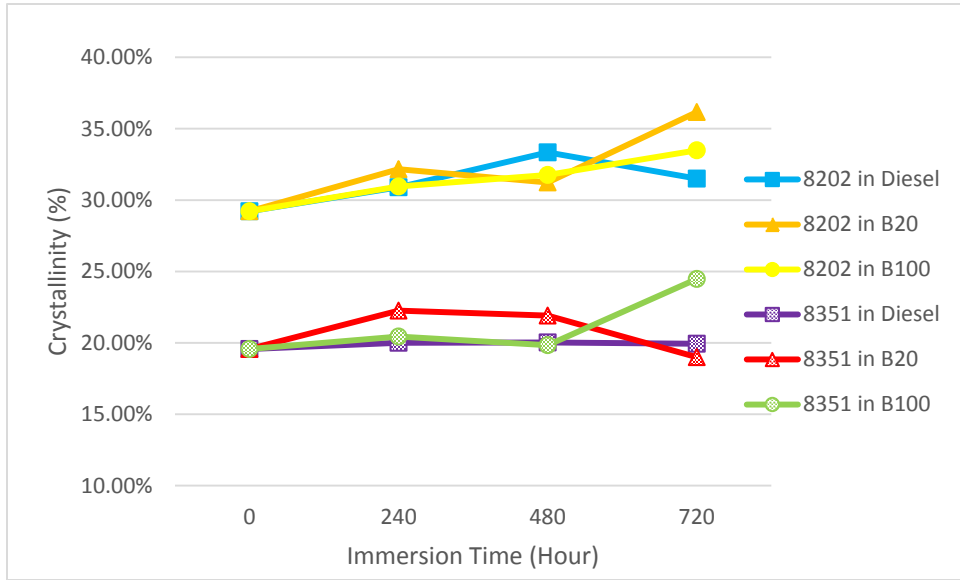


Figure 13: Variation of degree of crystallinity of Capron 8202 and 8351 as a function of immersion time

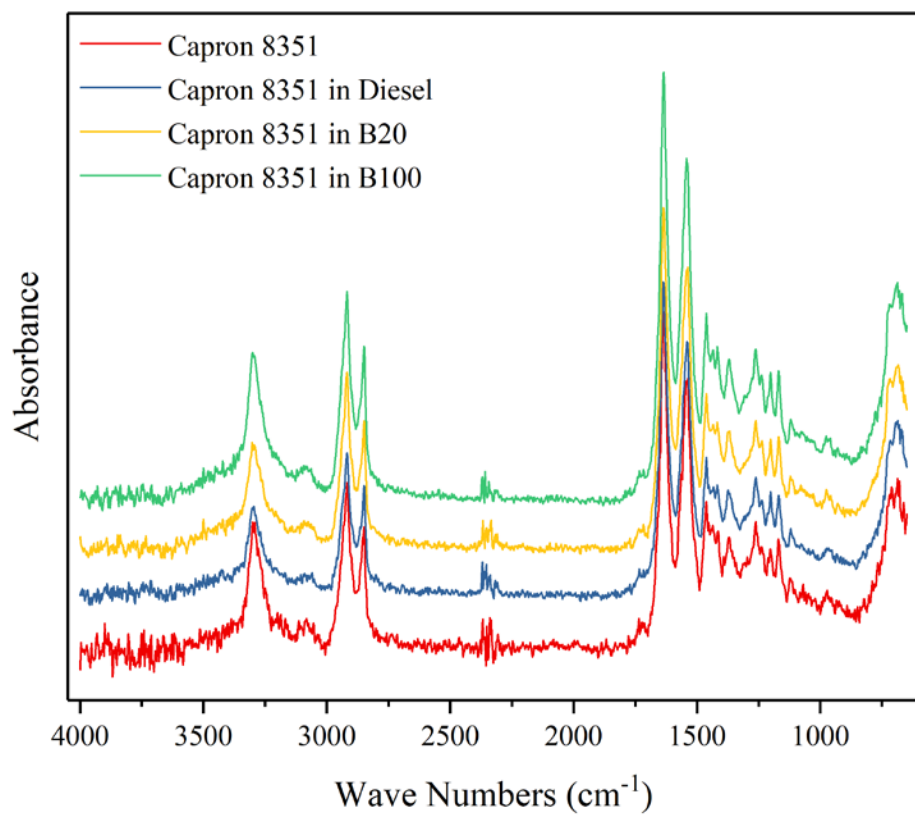
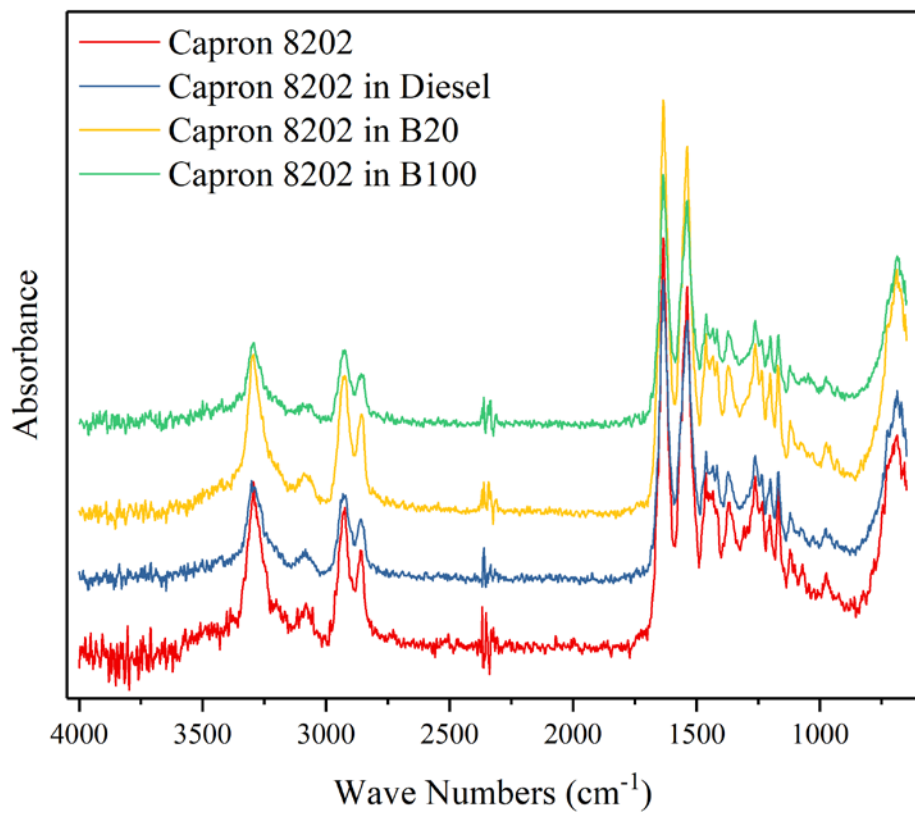


Figure 14: FTIR absorbance spectra of Capron 8202 and 8351 before immersion and after 720-

hour immersion

Author Manuscript

Table 1: Weight increase after 720 hours of immersion at 25°C

Fuel	Percentage Weight Increase after 720 Hours of Immersion ⁽¹⁾			
	Unstressed		Stressed	
	8202	8351	8202	8351
Diesel	1.439	1.377	1.560	1.312
B20	1.756	1.560	1.866	1.511
B100	2.041	1.643	2.231	1.753

(1) Average of 5 specimens for each condition

Table 2: Yield and tensile strengths of Capron 8202 and 8351 before and after 720-hr. immersion at 25°C ⁽¹⁾

Immersion Condition	Capron 8202		Capron 8351		
	Yield Strength (MPa)	Tensile Strength (MPa)	Yield Strength (MPa)	Tensile Strength (MPa)	
Before immersion	62.7	67.3	40.7	44.2	
After 720-hr. immersion @ 25 °C	DIESEL	59.7	64.5	38.6	42.5
	B20	58.2	65.1	36.4	37.8
	B100	58.4	64.5	38.5	43.1
After 720-hr. stressed immersion @25°C	DIESEL	56.0	64.7	34.8	37.7
	B20	54.5	63.3	32.7	37.4
	B100	51.5	61.0	34.0	39.1

(1) Average of 3 specimens for each condition

Table 3: T_g , peak $\tan \delta$, storage modulus and loss modulus of Capron 8202 and 8351 at 25°C

Material	Time of Immersion (Hour)	Condition		T_g (°C)	Peak $\tan \delta$	Storage modulus (GPa)	Loss Modulus (MPa)
Capron 8202	0	Dry		70.77	0.1254	1.835	0.0466
	After Immersion						
	720	25°C	Diesel	53.10	0.1049	1.372	113.400
	720	25°C	B20	46.65	0.1038	1.188	116.800
	720	25°C	B100	32.90	0.1029	1.239	121.500
	720 (Stressed)	25°C	Diesel	45.30	0.1142	1.377	130.460
			B20	32.05	0.1067	1.197	124.350
B100			30.55	0.1099	1.078	116.540	
Capron 8351	0	Dry		70.2	0.1303	1.314	0.0619
	After Immersion						
	720	25°C	Diesel	56.40	0.1176	1.134	92.500
	720	25°C	B20	57.35	0.1078	1.168	94.860
	720	25°C	B100	56.10	0.1078	1.215	92.100
	720 (Stressed)	25°C	Diesel	55.25	0.1235	0.967	91.703
			B20	56.15	0.1120	0.868	88.673
B100			56.25	0.1102	0.773	78.912	

Table 4: Degree of crystallinity and melting temperature of Capron 8202 and 8351 before and after 720-hr. immersion at 25°C

Immersion Time (Hour)	Immersion Condition		Capron 8202		Capron 8351	
			% Crystallinity	T _m (°C)	% Crystallinity	T _m (°C)
0	Before Immersion		29.23	223.61	19.57	221.63
720	25°C	Diesel	31.5	225.99	19.93	221.02
720	25°C	B20	36.17	223.98	18.99	221.28
720	25°C	B100	33.49	224.49	24.47	221.64
720 (Stressed)	25°C	Diesel	31.13	224.12	20.28	221.64
		B20	30.38	224.42	20.03	222.48
		B100	33.85	223.97	19.01	220.06

Table 5: FTIR wave numbers observed for Capron 8202 and 8351 before and after 720-hr. immersion at 25°C ⁽¹⁾

Standard Wave Numbers (cm ⁻¹)	Functional Group	Capron 8202				Capron 8351			
		Before Immersion	Diesel	B20	B100	Before Immersion	Diesel	B20	B100
3294	N-H stretching	3294	3302	3295	3294	3300	3295	3300	3300
3083	N-H stretching	3084	3083	3089	3094	3082	3085	3085	3085
2937	Antisymmetric CH ₂ stretching	2924	2932	2924	2922	2918	2919	2918	2918
2868	Symmetric CH ₂ stretching	2860	2859	2856	2857	2850	2850	2850	2850
1645	C=O stretching	1635	1635	1635	1635	1635	1635	1635	1635
1545	C-N stretching	1536	1536	1536	1536	1537	1541	1541	1541
1477	CH ₂ scissor vibration	1462	1460	1460	1460	1460	1460	1460	1461
1417	CH ₂ scissor vibration	1432	1417	1417	1417	1417	1417	1417	1417
1374	CH ₂ wagging vibration	1370	1370	1370	1370	1370	1374	1374	1370
1264	N-H bending & C-N stretching	1262	1262	1262	1262	1262	1262	1262	1262
1201	CH ₂ twist-wagging vibration	1202	1201	1202	1202	1202	1202	1202	1202
1170	CO-NH skeletal motion	1168	1168	1168	1168	1168	1168	1168	1168
960	C=O & N-H in-plane vibration	975	975	975	975	975	975	975	975
692	NH out-of-plane bending	690	688	688	688	686	685	685	686

(1) Immersion time 720 hours at 25°C